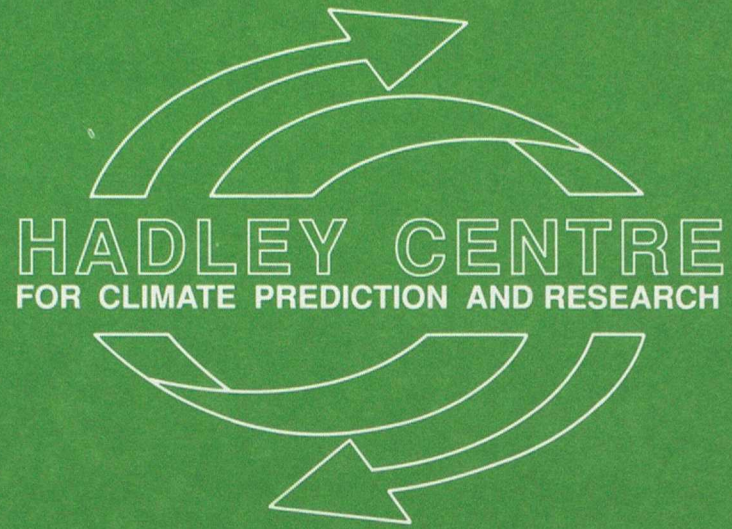

Empirical parameterisation of tropical ocean-atmosphere coupling

by

M. R. Allen, M. K. Davey, D. L. T. Anderson and P. D. Killworth

CRTN 22 December 1991

CLIMATE
RESEARCH
TECHNICAL
NOTE

Hadley Centre
Meteorological Office
London Road
Bracknell
Berkshire RG12 2SY

CLIMATE RESEARCH TECHNICAL NOTE NO. 22

EMPIRICAL PARAMETERISATION OF TROPICAL OCEAN-ATMOSPHERE COUPLING

by

Myles Allen, Michael Davey, David Anderson and Peter Killworth

Hadley Centre for Climate Research and Prediction
Meteorological Office
London Road
Bracknell
Berkshire RG12 2SY
U.K.

Note: This paper has not been published. Permission to quote from it should be obtained from the Director of the Hadley Centre

EMPIRICAL PARAMETERISATION OF TROPICAL OCEAN-ATMOSPHERE COUPLING: THE "INVERSE GILL PROBLEM"

Myles R. Allen[1], Michael K. Davey[2], David L. T. Anderson[1], *and* Peter D. Killworth[3]

1) Atmospheric, Oceanic and Planetary Physics, University of Oxford
Clarendon Laboratory, Parks Road
Oxford OX1 3PU, UK

2) Meteorological Office Unit
Robert Hooke Institute, Clarendon Laboratory, Parks Road
Oxford OX1 3PU, UK

3) Institute of Oceanographic Sciences, Wormley, UK
and Robert Hooke Institute, Clarendon Laboratory, Parks Road
Oxford OX1 3PU, UK

EMPIRICAL PARAMETERISATION OF TROPICAL OCEAN-ATMOSPHERE COUPLING: THE "INVERSE GILL PROBLEM"

Myles R. Allen, Michael K. Davey, David L. T. Anderson and Peter D. Killworth

Abstract

A number of linear models of the steady-state response of the tropical atmosphere to sea-surface temperature (SST) anomalies have been proposed, all based on the shallow-water equations. Despite their formal similarity, the various models have very different physical interpretations, and suggest widely varying values for key parameters, including the mechanical damping rate (or coefficient of Rayleigh friction), the strength of the coupling to SST and the "effective stability" of the lower troposphere. In order to place empirical constraints on these coefficients, the linear momentum equations are inverted to obtain the scalar forcing fields P' (interpreted as vertically-integrated boundary-layer pressure anomalies) which best reproduce observed surface wind anomalies through the period 1984-90. This gives an optimum value for the mechanical damping rate, independent of the coupling parameterisation. Direct optimisation of a fully linear "Gill-type" model of ocean-atmosphere coupling reveals that the problem of identifying optimum values for the other two parameters (coupling and stability) is degenerate: if one parameter is fixed, the other is well constrained by the data, but if both are allowed to vary, the cost function (r.m.s. error in the model output winds) has no well-defined minimum. However, models of this type also suggest a simple relationship between P' and anomalies of SST and divergence. A significant but strikingly different relationship is found between these three quantities derived from the observations. If uniform, linear coupling is assumed, this result suggests that the large-scale response of the tropical atmosphere to SST anomalies is consistent with a moderately moist-unstable boundary layer, with the stability of the response being maintained by turbulent diffusive processes. This may be parameterised most simply by introducing biharmonic diffusion on P' into the "thermodynamic" equation of a Gill-type model. Simple forms of non-linear coupling both to SST and to divergence are also investigated. Although the possibility that non-linear effects are important cannot be excluded, no evidence is found to suggest that either of two widely-used non-linear coupling parameterisations represent an improvement on a fully linear scheme.

1) Background

Diagnostic models of the equilibrium, steady-state response of the tropical atmosphere to SST and diabatic heating anomalies are widely used in studies of low-latitude ocean-atmosphere coupling. Such models are generally based on the linear shallow-water equations, interpreted in one of two ways: either as the first baroclinic mode response of the full tropical troposphere to external forcing (primarily diabatic heating due to latent heat release), this being the original interpretation proposed by Matsuno (1966) and Gill (1980) and developed by Zebiak (1986) and Zebiak & Cane (1987) (ZC hereafter); or as a boundary-layer response to sensible heating due to sea-surface temperature gradients, as proposed by Lindzen & Nigam (1987) (LN). More complex models, such as those of Davey and Gill (1987), Neelin (1988) and Kleeman (1991) also use the linear shallow-water equations, their additional complexity arising from the way they parameterise the relationship between the atmospheric forcing Q' and the SST and surface convergence. Thus although this study will focus on the models of ZC and LN, the overall approach may have wider application for model-data comparison.

Neelin (1989) has shown that both interpretations may, with some simplification, be cast in the following form:

$$r_m U' - \beta y V' = -P'_x \qquad (1)$$

$$r_m V' + \beta y U' = -P'_y \qquad (2)$$

$$r_t P' + c^2 D' = -Q'(T,T',D,D') \qquad (3)$$

where U and V are the surface winds, D is the surface divergence and T the sea-surface temperature. Primes indicate anomalies about the mean annual cycle. In this simplified formulation, Q' represents the combined effect of sensible and latent heating. It is conventionally taken to be a function of the local (total and anomalous) divergence and SST, which takes into account possible non-linear coupling to SST and non-linear convergence-forcing feedback.

Equations *(1)* to *(3)* represent the equilibrium response to mean forcing over time-scales longer than the characteristic atmospheric adjustment time: time-derivatives are thus replaced by constants of mechanical damping, r_m, and "Newtonian cooling", r_t. By scaling all terms in *(3)* by r_t/r_m, we may set $r_m = r_t = r$ hereafter. The physical interpretation of the

terms in *(3)*, and thus of P' and the coefficient c^2, depends on the overall interpretation of the model, discussed below.

The formal similarity of the various models, in contrast to their different physical interpretations, suggests two questions to be investigated here. First: how well do observed winds in the tropics satisfy the basic damped shallow-water model, before any assumptions are introduced concerning ocean-atmosphere coupling (i.e. how close a fit to the observations can be obtained allowing the external forcing Q' in *(3)* to take any form)? This question has already been addressed by Zebiak (1990) (Z hereafter) using a slightly different approach. Second: how can Q' best be parameterised in terms of local divergence and SST? This will be investigated by fitting the model to the large-scale data without making any assumptions concerning the micro-physics of ocean-atmosphere interaction. Here the conclusions of this study differ in important respects from those of Z.

2) Inverting the linear momentum equations

The first step is to invert the linear momentum equations *(1)* & *(2)* to obtain "vertically integrated boundary-layer pressure anomaly" fields P' which, when inserted into the right-hand-side of these equations, generate the "best" (minimum r.m.s.) fit to observed surface wind anomalies. Since Q' may take any form, *(3)* does not introduce any further constraint on the model, and is therefore not required at this stage. The physical interpretation of P' need not concern us either. Since the differences between the models mentioned in section 1 concern either equation *(3)* or the physical interpretation of terms, this initial investigation is relevant to all of them.

We define "best fit" by minimising the cost function

$$C_1(P',r) \equiv \sum w(y)[(U' - U^{0\prime})^2 + (V' - V^{0\prime})^2] \qquad (4)$$

where U', V' and P' satisfy the linear momentum equations *(1)* and *(2)*, $U^{0\prime}$ and $V^{0\prime}$ are observed zonal and meridional wind anomalies, and $w(y)$ is a statistical weighting function. In principle, minimising C_1 may be thought of as an unconstrained optimisation problem, involving adjusting the elements of P' and the damping constant r, since if these are specified, the (U',V') field is uniquely defined by equations *(1)* and *(2)*.

In practice, it is easier to regard the linear momentum equations as representing a constraint on allowed wind fields, which is most clearly seen by taking the curl of *(1)* & *(2)* to obtain the linear vorticity balance condition

$$r(V'_x - U'_y) + \beta y(U'_x + V'_y) + \beta V' = 0. \qquad (5)$$

Identifying the wind field (U',V') which minimises C_1 and satisfies *(5)* then becomes a constrained optimisation problem, which may be solved using Lagrange multipliers (see appendix 1 for details). The boundary conditions applied were $V' \equiv 0$ on the northern and southern boundaries. Other boundary conditions were also investigated (appendix 1) but the choice was found to have little effect on results. Zonal mean quantities require special treatment. Once the best-fit (U',V') field has been obtained, P' may be found, to within an integration constant, by integrating either *(1)* or *(2)* (the (U',V') field, by definition, satisfies both).

We applied a meridional weighting function $w(y)$, with a half-width at half-maximum of 5° latitude, giving greater statistical weight to wind observations near the equator. In the context of ocean-atmosphere coupling, it is widely accepted that winds within the oceanic equatorial waveguide region play the largest role in determining interannual variability (Hirst - 1986). Equal weight was also given to zonal and meridional winds, although the technique would allow for differential weighting. Because the residuals turn out to be small, the statistical weights chosen have very little effect on the resulting fields. This procedure may be thought of as applying a simple dynamical filter to wind data. In what follows, "filtered winds" refers to solutions to the linear momentum equations which have been fitted to observational data in this way.

Z addressed the same problem using a different technique. He solved for P' using *(1)* on a reference latitude; integrated away from that latitude using *(2)*; repeated for all possible reference latitudes; and then averaged the fields thus obtained. Our approach involves less computation, guarantees a minimum-variance fit to an arbitrary wind field and allows for greater transparency and flexibility in the use of statistical weighting. However, if the residuals are small (which, in the data-set considered, they are) the two techniques should give very similar results.

The data used were 1000 mb monthly mean winds obtained from the European Centre for Medium-Range Weather Forecasting operational analysis forecast system, for the period

July 1984 to June 1990, averaging the 0 and 12 hour analyses. In order to minimise the model-dependence of the data-set, the data had not been subjected to prior "initialisation" (a filtering procedure to remove dynamical features which would, in the ECMWF model, have led to the development of fast-propagating gravity waves). Nevertheless, any analysed wind field in this data-sparse region must be presumed to have a strong model content. The ECMWF wind data-set was felt to be the best available with a global coverage for this period. The short time-series considered (72 months) means that all results are dominated by the strong anomalies which occurred during the "El Niño" and "La Niña" years 1987 and 1988: thus all the following conclusions may be specific to that particular El Niño/Southern Oscillation (ENSO) "cycle". It would be necessary to consider a longer data-set before drawing general conclusions concerning ENSO time-scale anomalies.

A mean annual cycle was calculated for the series, and anomalies $(U^{0\prime},V^{0\prime})$ calculated about it. The data was obtained on a 1°x1° grid, interpolated to a 2°(zonal)x1°(meridional resolution) grid for the calculation of U', V', P' and D'. Output U', V', P' and D' fields and SST anomalies were interpolated to a 6°x4° grid for statistical analysis. None of the results were found to be sensitive to the choice of grid resolution.

The value of r found to minimise C_1 using the above procedure was $1.0*10^{-5}s^{-1}$, corresponding to a mechanical damping rate of about $(1\ day)^{-1}$. This value is consistent with that found by Z, who was investigating FSU data (Goldenberg & O'Brien - 1981). The same calculations carried out on ECMWF 850mb winds gave a smaller optimum damping rate $(3.6*10^{-6}s^{-1})$, but otherwise gave similar results in all that follows. 1000 mb results are presented here, since the overall objective is to investigate linear models for surface winds.

Equatorial zonal wind anomalies about a mean annual cycle for 1984 – 90 from the ECMWF analysis are shown in figure 1a. Figure 1b shows the filtered winds (the best fit to equations *(1)* & *(2)* with this optimum value of r) and fig. 1c shows the residual. The r.m.s. "error" (the component of the observations excluded by the dynamical filter) over the whole region is small $(< 0.4ms^{-1})$, indicating that the linear momentum equations are almost exactly satisfied by the ECMWF analysed winds throughout this period.

However, maximum errors occur in precisely the region (the West Pacific) where they are expected to be important for coupled ocean-atmosphere phenomena. Zonal wind anomalies in the filtered winds are weaker than the ECMWF analysed wind anomalies in this region

by about $1ms^{-1}$ in both phases of the 1986-88 ENSO cycle. No coherent pattern is discernible in the equivalent meridional "error" field. Constraining winds to fit the linear momentum equations seems to have the effect of slightly reducing the strength of equatorial zonal wind anomalies. It will be assumed hereafter that this effect is small enough to be unimportant, but it must be borne in mind if our results are to be applied to coupled modelling: slightly stronger (by 15 to 20%) coupling might be appropriate than that suggested by the analysis of filtered winds, to compensate for the fact that the filtered wind anomalies are weaker than the observations by approximately this amount.

Comparison of these results with those of Z suggests that the r.m.s. error excluded by the dynamical filter from the ECMWF wind data-set is smaller than that which it excludes from the FSU winds (Z reports an r.m.s. error of $< 1ms^{-1}$). This is to be expected, because a certain level of dynamical consistency has already been imposed on the ECMWF data by the operational analysis system, even though un-initialised winds have been used. If we believe that recent ECMWF data constitute on average a "better" representation of the true winds than the FSU data-set, this result supports Z's proposal that FSU and other long data-sets should be subjected to such a dynamical filtering procedure before use in modelling studies. An exact comparison should be carried out to confirm this observation.

Having obtained the best-fit wind field, the corresponding P' field (figure 2a) may be found by integrating *(1)* or *(2)*, and the divergence D' (figure 2c) by differentiating the filtered winds. As an integrated field, P' is substantially smoother than the wind fields used to generate it. It will therefore contain a stronger signal-to-noise ratio for phenomena of interest, provided they have a longer spatial scale than the characteristic scale of the noise. It thus may provide better "raw material" for pattern-recognition studies (such as principal oscillation pattern analysis after Xu & Storch (1990)) than the unfiltered wind data. This is to be pursued in a subsequent study. Except for being somewhat smoother, P' appears very similar to the surface pressure field inferred from the ECMWF 1000 mb geopotential height and temperature fields.

Equatorial SST anomalies T', from the Climate Analysis Centre (CAC) dataset of monthly mean SSTs (Reynolds - 1988), are shown in figure 2b. Comparing figures 2b and 2c suggests that divergence and SST anomalies are fairly strongly anti-correlated. Thus identifying an optimum regression model for P' in terms of T' and D' may present problems of degeneracy. In geometric terms, P' is being projected onto two vectors which are almost parallel. This explains why such widely varying parameter values have been

proposed in the past on the basis of essentially the same observations: adopting a larger value of c^2 may be largely compensated for by adopting stronger coupling to SST and *vice-versa*. This effect is most clearly seen in our attempt to optimise a linear model directly, discussed next.

3) Direct linear model optimisation

Surface wind observations in the tropics, to a good approximation, satisfy the linear damped momentum equations. However, these are not enough for a useful atmosphere model: a third equation is required, relating the winds (or P')to external boundary conditions. This is the "thermodynamic" equation *(3)* above. Its simplest form assumes a linear relationship between the external forcing Q' and the SST – this is approximately the relationship used by LN:

$$rP' + c^2D' \quad = \quad -Q'_{(LN\ model)} \quad \equiv \quad -k_qT', \qquad (3a)$$

where k_q is the coupling coefficient, and c^2 (in the LN model) is proportional to the delay in the cumulus flux removing excess mass from the atmospheric boundary layer. *(3a)* is not specific to the LN boundary-layer interpretation. First-baroclinic-mode interpretations such as that of ZC propose a similar relationship between P', D' and T'

$$rP' + c^2D' \quad = \quad -Q'_{(ZC\ model)} \quad \equiv \quad -k_q[f_T(T-28°C)]' + c^2[(1-f_D)D]'. \qquad (3b)$$

In the ZC model $c^2 \equiv c_d^2$, the "dry" static stability (parameterising the stabilising effect of cooling (warming) due to the upward (downward) motion of air in the absence of moist processes). The second term on the RHS represents the effect of latent heating due to moisture-convergence feedback. f_T and f_D are non-linear functions of the divergence and SST respectively. The primes outside the square brackets in *(3b)* indicate that T and D are multiplied by f_D and f_T before anomalies are calculated about the annual cycle. This does not prevent $[(1-f_D)D]'$ from being expanded, simplifying *(3b)* thus

$$rP' + c^2[f_DD]' \quad = \quad -k_q[f_T(T-28°C)]'. \qquad (3c)$$

In the standard ZC model, f_D and f_T have approximately the following form:

$$
\begin{aligned}
f_D = a_D &= (1-\beta_z) = 0.25 \quad \text{for total } D<0 \\
&= 1 \quad \text{for total } D>0 \\
f_T \approx a_T &= 0.8 \quad \text{for total } T<28^{\circ}C \\
&\approx 1 \quad \text{for total } T>28^{\circ}C
\end{aligned}
$$

β_z will be recognised as Zebiak's convergence feedback parameter and f_T is a simplified version of his exponential coupling to SST, linearised about $26.5\,^{\circ}C$ and $29.5\,^{\circ}C$. However, these are not the only functional forms of f_T and f_D which are consistent with the first-baroclinic-mode interpretation of the model. The exponential form of $(f_T T)$, justified in the ZC model by the Clausius-Clapeyron relation, might be considered an upper limit on the strength of the non-linearity of coupling to SST, since any coupling due to sensible heating could be closer to linear. Even at this limit, the model is not particularly non-linear over the range of temperatures of interest, as may be seen by the fact that the value of f_T is close to *1* for all T: thus linear coupling to SST $(a_T = 1)$ could be compatible with this interpretation.

There might seem to be more physical justification for the non-linear form of f_D, since it could be argued that if the total flow is divergent no convergence-induced latent heating can occur, and therefore any reasonable parameterisation of this process must contain some type of step-function similar to f_D above. This argument is not conclusive, for the following reason. Provided that the sub-grid-scale variability in the divergence field is significantly larger than its large-scale variability (as may well be the case), then even if the overall flow in a grid box is divergent, convergence will always be occurring somewhere within it. The intensity of convergence-induced latent heating could, in this picture, be governed by the proportion of the grid-box area in which the flow is convergent. This proportion may never fall to zero, removing the motivation for a step function in the latent heating parameterisation. $f_D c^2$ would then have some constant value less than c_d^2 for all values of D'. In this case we can simply allow $c^2 < c_d^2$, set $a_D = 1$, and *(3c)* reduces to *(3a)*. *(3a)* may therefore be relevant to both interpretations of the model, with c^2 being understood as the effective moist static stability of the troposphere (i.e. the stability including the effect of latent heating) in the first-baroclinic-mode interpretation.

Together, *(1)*, *(2)* and *(3a)* represent a linear but non-local function G relating wind to SST anomalies. For a given SST anomaly field T', and given values of c^2, k_q and r, the solution winds $U'' \equiv (U'', V'')$ may be found using the method described in Gill (1980). SST values in the CAC dataset are interpolated over land by solving Poisson's equation

with zero forcing, anchored by coastal SSTs (Reynolds – 1988): the problem of missing SST data over land may thus be avoided by using these interpolated values. In effect, this means assuming that forcing over land may be inferred by interpolation between marine forcing values adjacent to the coastlines, which seems a reasonable approach for the optimisation of such a simple linear model.

An optimum value of the mechanical damping rate r has already been identified in section 2. Since T' is given by the observations, the model has only two free parameters: the coefficients c^2 and k_q. Thus

$$U'' \equiv G(T',c^2,k_q). \qquad (6)$$

Optimum values of k_q and c^2 may be found by minimising the cost function:

$$C_2(c^2,k_q) \equiv \sum w(y)[(U'' - U')^2 + (V'' - V')^2] \qquad (7)$$

applying the meridional weighting function w as above. In practice, finding the minimum of C_2 may be simplified because the model scales exactly with k_q. *(6)* can therefore be recast thus:

$$U'' \equiv k_q G(T',c^2,1). \qquad (6a)$$

We thus assumed a particular value for c^2, and solved G given T' and a coupling coefficient of unity. The optimum value of k_q corresponding to that value of c^2 was then found by linear regression (solving for the value of k_q for which $\partial C_2/\partial k_q = 0$).

Note that *(7)* implies fitting to the filtered wind fields (U',V') obtained in section 2 as the best fit to the linear momentum equations. It might be argued that it would make more sense to fit to the original wind observations. Which approach is preferred depends on whether the residual wind field shown in figure 1c is interpreted as noise (in which case it would be undesirable for a linear model to try to capture it), or an important component of the signal (which the model should attempt to represent). For a "good" data-set such as the one used here, the latter interpretation might make the most sense. However, for consistency with subsequent work using lower quality data, results are given here from fitting the model to the filtered winds. Since the difference between the filtered and original wind fields is so small, which approach is taken has no significant effect on the results.

Figure 3a shows how the optimum value of k_q varies with the value chosen for c^2. The relationship is clearly linear, with the only point not lying on the regression line being $c^2 = 10m^2s^{-2}$, which should be treated with caution in any case, since it is close to the limits of stability of the model (which becomes unstable for $c^2 < 0$).

The standard errors of the estimates for k_q shown in figure 3a are indicative only, since they depend on a rather crude algorithm (discussed in appendix 2) used to estimate the number of degrees of freedom (DOF) of the system, which is, in effect, the number of independent observations used to calculate each value of k_q. Wind data on adjacent grid-points are not, of course, independent, so the total DOF is substantially less than the number of data-points and not particularly well defined. However, the only conclusion to be drawn from figure 3a is that, given a value for the effective moist stability (or cumulus-uptake-time) c^2, the data suggest a sensible optimum value for the coupling coefficient k_q, and that there is a clear relationship between this value found for k_q and the value assumed for c^2. Quantitatively, this has the form (recalling $r = 1*10^{-5}s^{-1}$):

$$k_q = [2.6*10^{-4} + 3.2*10^{-7}(c^2)]m^2s^{-3}K^{-1} \qquad (8a)$$

or, if the point $c^2 = 10m^2s^{-2}$ is omitted from the regression,

$$k_q = [4.3*10^{-4} + 2.7*10^{-7}(c^2)]m^2s^{-3}K^{-1}. \qquad (8b)$$

The value of c^2 proposed by LN is (after scaling to the mechanical damping rate used here) $540m^2s^{-2}$. This gives optimum values for k_q of 4.3 or $5.7*10^{-4}m^2s^{-3}K^{-1}$, depending on which regression line is used. These values may be compared with their proposed coupling coefficient of $5.1*10^{-4}m^2s^{-3}K^{-1}$, which is based on physical arguments concerning the mean structure and dynamics of the boundary layer (boundary-layer depth of $3000m$, linearisation temperature of $288K$, mechanical damping rate of $1.0*10^{-5}s^{-1}$ and cumulus uptake time of $30min.$ – calculation based on Neelin (1989)).

None of the other models mentioned in section 1 may be approximated by purely linear coupling, so they cannot be compared directly with this regression-based model. Nevertheless, it is interesting that all use values of c^2 substantially higher than that proposed by LN (by up to a factor of 6), and also use substantially stronger coupling (by more than an order of magnitude – although the fact that their coupling is non-linear makes

a quantitative comparison of limited value). This would suggest that the functional dependence of k_q on c^2 has been noted by these authors, even if it has not been stated explicitly.

Unfortunately, this simple approach clearly fails to identify an optimum *combination* of parameters. Figure 3b shows how the r.m.s. error in the wind field (or the square root of the cost function C_2) varies with c^2. It illustrates graphically the problem of degeneracy mentioned at the end of the previous section: the r.m.s. error in the equatorial wind fields changes by less than 5% as c^2 varies from close to zero to $6000 m^2 s^{-2}$, and k_q varies by more than an order of magnitude. Provided the coupling to SST is adjusted appropriately, the model error is clearly not sensitive to the value of c^2 in *(3a)*.

One of the key differences between the boundary-layer model of LN and first-baroclinic-mode models, such as ZC, is the characteristic length-scale of the response (given by c/r). LN propose a relatively short spatial scale, i.e. a small value of c and correspondingly weak coupling coefficient k_q. Other models propose larger values of c and stronger coupling. Because of the problem of degeneracy, simply optimising the fit between model output and observed winds fails to identify a preferred spatial scale, although it does indicate that if one of these constants is set by some independent physical argument, the other is relatively well constrained by the data. To identify the "better" model, other approaches are required, and some alternatives are discussed below.

Before leaving the discussion of direct model optimisation, one further result should be mentioned. The effect of the introduction of non-linear coupling to SST was investigated by repeating the above optimisation exercise using *(3c)* in place of *(3a)*, with linear coupling to divergence ($f_D = 1$ for all values of D), and non-linear coupling to SST ($f_T = 1$ for $T > 28°C$ and $f_T = a_T$, an adjustable constant less than *1*, otherwise). The value of a_T sets the strength of the non-linearity: $a_T = 1$ corresponds to fully linear coupling. Such a scheme, with strongly non-linear coupling ($a_T = 0$), is used in the coupled model of Anderson & McCreary (1985).

Introducing non-linear coupling to SST in this way was found to increase the r.m.s. error in the model output, even for values of a_T close to *1*. While there is clearly still a need to investigate this type of non-linearity (we return to it below), this simple approach fails to provide any direct evidence in its favour in this data-set.

4) Evidence from spatial patterns

Z proposes an alternative method of distinguishing between the LN and ZC models by inspecting spatial patterns in "heating fields" Q' which he obtained as follows. He generated P' and D' fields from wind observations by inverting the linear momentum equations, and then constructed "inverse model" Q' fields using *(3)*, thus

$$Q'_{(inverse\ model)} \equiv -rP' - c^2D', \qquad (9)$$

introducing the subscript on Q' to indicate how it has been derived.

Z noted that at a time when anomalies were near their peak, such as January 1987, the spatial structure of $Q'_{(inverse\ model)}$ (assuming, with Z, that $c^2 = c_d^2 = 3{,}600 m^2 s^{-2}$ – figure 4a) was very similar to the large-scale convergence, $-D'$, and to quantities which are well correlated with $-D'$ such as outgoing longwave radiation and highly reflective cloud anomalies. This, he argued, was evidence in favour of the coupling mechanism proposed in the ZC model which, slightly simplified, states that the anomalous forcing due to a given SST and large-scale convergence field may be represented by $Q'_{(ZC\ model)}$ as defined in *(3b)* above. An optimum value of k_q may be found by minimising the r.m.s. difference between $Q'_{(inverse\ model)}$ and $Q'_{(ZC\ model)}$. The January 1987 $Q'_{(ZC\ model)}$ field with this value of k_q is shown in figure 4b.

In the region of interest, the West and Central Pacific, the fields shown in figures 4a and 4b have a very similar spatial structure. However, this may not be conclusive evidence in favour of the ZC model for the following reason. P' is substantially smoother than D' (cf. the January 1987 P' field shown in figure 3c) and almost flat in the Central Pacific, where Z focused attention. So the spatial structure of $Q'_{(inverse\ model)}$ will be dominated by D' unless c^2 is very small. Since the total flow was convergent over most of the region of interest in January 1987, convergence feedback was active. Thus $(1 - f_D) \neq 0$ in *(3b)*, and therefore the structure of $Q'_{(ZC\ model)}$ is also dominated by D'.

The structure of both $Q'_{(inverse\ model)}$ and $Q'_{(ZC\ model)}$ are therefore, by construction, dominated by the same field, so it is not clear if their visual similarity is significant. The following argument suggests it may even be misleading. To a good approximation, the only differences between the LN and ZC models are the different values they adopt for the

parameters k_q and c^2 (recall $c^2 \equiv c_d^2$ in the ZC model, because ZC specify no latent heating in regions of divergent flow), and the forms they adopt for the functions f_T and f_D. Z's argument can therefore be formalised in terms of minimising the cost function

$$C_3(c^2,k_q,a_T,a_D) \equiv \sum w(y)[Q'_{(inverse\ model)} - Q'_{(forward\ model)}]^2. \qquad (10a)$$

$Q'_{(forward\ model)}$ is a "universal" heating parameterisation, defined in exactly the same way as $Q'_{(ZC\ model)}$, but with c^2, k_q, a_T and a_D now allowed to take any value. $Q'_{(inverse\ model)}$ is defined as in *(9)*. Specifying that c^2 has the same value in $Q_{(inverse\ model)}$ and $Q'_{(forward\ model)}$ does not represent a constraint, since a_D is allowed to vary: a model with different values of c^2 on the LH and RH sides of *(3b)* will always be exactly equivalent to one with a single value of c^2 and a different value of a_D. Equation *(3b)* with $Q'_{(forward\ model)}$ on the RHS thus encompasses both the LN and ZC models, so finding the parameter set (c^2,k_q,a_T,a_D) which minimises C_3 seems a reasonable way of distinguishing which is the better model.

Recalling the expansion of the third term in *(3b)*, *(10a)* is equivalent to

$$C_3(c^2,k_q,a_T,a_D) \equiv \sum w(y)[rP' + c^2D'^{(I)} + k_q[f_T(T-28°C)]' - c^2D'^{(II)} + c^2[f_D D]']^2. \qquad (10b)$$

Since $D < 0$ over most of the region of interest, $f_D = a_D$. If, following Z, a value is assumed for a_D which is significantly less than *1* (Z assumes $a_D = 0.25$), then the terms dominating the spatial structure of $Q'_{(inverse\ model)}$ and $Q'_{(forward\ model)}$ will be the terms labelled *(I)* and *(II)* in *(10b)*, which cancel each other. Hence comparing spatial patterns of $Q'_{(inverse\ model)}$ and $Q'_{(forward\ model)}$ with a small value presupposed for a_D is unlikely to yield information on parameter choices which minimise C_3, and may be misleading.

Z remarks that the spatial pattern of $Q'_{(inverse\ model)}$ will still resemble the divergence field even if c^2 is as small as proposed in LN. While this is true, it may simply be a consequence of the different scales of spatial structure of the P' and D' fields (discussed above), making it difficult to interpret. If it does indicate a shortcoming in the LN model, it suggests their stability parameter c^2 may be too large. There is little evidence in the visual appearance of the P' and D' fields inferred from observed winds to indicate such a value of c^2 in the first place. P' in figure 3c, along the equator at least, resembles the SST anomaly (figure 3d) much more than it does the D' field (which appears identical to figure 3a).

Physically, Z's argument may be summarised as showing that the optimum value of the effective moist stability ($a_D c^2$ in regions of convergent flow) is substantially less than the value he assumes for the dry stability c_d^2: i.e. in a first-baroclinic-mode picture, moist processes reduce the stability of the tropical troposphere. While probably true, this is unsurprising. It also does not necessarily show that moist processes are important, because the first-baroclinic-mode picture has not been shown to be necessarily correct. LN have shown that it is possible to justify a much smaller value of the stability parameter in a boundary-layer interpretation, without invoking moist processes. The crucial question in distinguishing between the LN and ZC mechanisms, finding the optimum values of c^2, k_q, a_T and a_D, remains unresolved.

5) Regression analysis

Inspecting patterns in composites made up of fields with very different scales of spatial structure may be misleading. However, attempting to find values of c^2 and k_q, and forms for the functions f_T and f_D, which minimise the cost function C_3 nevertheless seems a reasonable approach to optimising a coupling parameterisation.

The linear coupling case, in which f_T and f_D are constant for all values of T and D ($a_T = a_D = 1$), will be investigated first. The model to be optimised is then *(3a)*, with P' and D' both derived from the filtered winds, and T' given by the SST observations. The cost function becomes

$$C_3(c^2,k_q) \equiv \sum w(y)[rP' + k_qT' + c^2D']^2. \qquad (10c)$$

A value for r has already been identified. So if linear coupling is assumed, optimum values for the other two parameters may be found by minimising C_3. Before proceeding to results, it is important to clarify the principle behind this approach, and how it differs from that taken in section 3. Models of the tropical atmosphere assert a non-local relationship between wind and SST anomalies. Minimising the r.m.s. error in their output winds fails, however, to distinguish between linear coupling models (and might well fail in the case of non-linear models as well). Provided they lie on or near the regression line shown in figure 3a, all linear models of this type do equally well on this criterion.

But these models might be considered to assert more than just the pattern and amplitude of the wind response to SST anomalies. *(3a)* states a local, linear relationship between simultaneously-occurring values of P', D' and T'. If all three of these variables signify physical quantities (as most of the literature on linear model atmospheres would appear to accept), then a model which gets the relationship between them "right" (closer to the relationship found in the observations) might be considered to be a "better" model than one which gets it "wrong", even if they both give similar r.m.s. errors in their output winds.

P' is only defined to within an arbitrary integration constant. Thus all area-means must be removed before quantitative comparisons may be made between P' and other fields. This may appear to conflict with investigating a local regression model by introducing non-local causal interactions: if the SST anomalies are confined to the East Pacific, for example, removing the area-means from the SST fields appears to "create" an SST signal in the West Pacific, in anti-phase with the East Pacific signal, where no signal was before. In the linear coupling case this does not matter: the winds respond to gradients of P' and Q', not to their area-means. When investigating possible non-linearities, however, it is important that area-means are removed after non-linear effects are taken into account.

If c^2 is fixed at $540 m^2 s^{-2}$ as in the LN model, minimising C_3 gives an optimum value of k_q of $5.9(+/-0.9) m^2 s^{-3} K^{-1}$, in agreement with their value and the results of the fitting-directly-to-winds approach taken in section 3. However, as in section 3, the optimum value of k_q is found to depend on the value chosen for c^2. Because the divergence and SST fields are broadly anti-correlated, a higher value of c^2 in *(10c)* may partially be compensated for by stronger coupling to SST. To identify the optimum combination of parameters, and thus the optimum scale length of the response, values of k_q and c^2 which minimise C_3 must be found simultaneously. This is again a simple regression problem, now with two independent variables, T' and D', and one dependent variable, rP'. As in section 3, it may be solved by identifying the values of c^2 and k_q for which $\partial C_3/\partial k_q = \partial C_3/\partial c^2 = 0$.

Before proceeding to quantitative regression analysis, it is essential to visualise how P' varies with D' and T'. Because all three variables are correlated, a simple two-dimensional scatter plot is inadequate. Figures 5a to 5c attempt to show a scatter plot in three dimensions. The P' axis is perpendicular to the page, with T' the horizontal and D' the vertical axis. 5a shows the number of samples (there being $N*M$ samples in total, where N is the number of grid-points and M is the number of months) in which T' was within $+/-0.05\,°C$ of the value on the horizontal axis, and D' was within $+/-2*10^{-7} s^{-1}$ of the value on

the vertical axis. In effect, the (T',D') plane is subdivided into *400 (0.1°C by $1*10^{-7}s^{-1}$)* rectangles, and the data binned accordingly. Fig. 5b shows the mean of P' among the samples at the corresponding point (in the appropriate bin) in fig. 5a. 5c shows the standard deviation of P' about that mean. Fig. 5b may be thought of as a surface passing through the mean (calculated perpendicular to the page) of the 3-D scatter plot, with fig. 5c indicating the spread of points and fig. 5a the density.

For a given value of D', P' decreases with T', as both LN and ZC models suggest it should. For a given T', however, P' appears to *increase* with D', (the surface slopes from lower right to upper left) which is the opposite of the relationship assumed in *(3a)* and in all of the simple models considered. It suggests that the value of the coefficient c^2/r which minimises the cost function in *(10c)* may be negative.

Quantitative analysis (fitting a plane surface to the "scatter plot" shown in figure 5) gives an optimum value of k_q of $(2.5(+/-0.35)*10^{-4}m^2s^{-3}K^{-1})$, and an "optimum" value of c^2 of $-27(+/-10)m^2s^{-2}$. This unexpected sign clearly indicates that the relationship observed in this dataset between P', D' and T' is not that which is suggested by *(3a)*.

Again, attempting to quantify the significance of these results is difficult because the total DOF of the system being analysed is not well defined. One statistic which is independent of the DOF is the coefficient of multiple correlation (CMC). This does not assign confidence limits to regression coefficients, but is simply a measure of the strength of the relationship between the variables. In this case, it has a value of 0.44, indicating a moderately but not particularly good correlation: as may be seen from the spread of points in figures 5b and 5c.

An estimate of the DOF of the system may be obtained by investigating the structure of the residual fields, discussed in appendix 2. This suggests that the system has only about 5 true DOF (5 independent observations) per monthly mean field, which is clearly conservative. Even on this basis, the standard errors of the estimates for k_q and c^2 given above suggest that both are significantly different from zero at the 95% level.

Thus there is a small (less than 5%) possibility that the relationships observed in figures 5a to 5c have occurred purely by chance. However, it remains possible that they may be misleading, for two reasons. First, the assumption of a linear model *(3a)* used in the definition of the cost function *(10c)* may be inappropriate. In that case, it is the relationship

between P', $[f_T(T - 28°C)]'$ and $[f_D D]'$ which should be investigated, with f_T and f_D reintroduced as non-linear functions of SST and divergence respectively. A preliminary investigation in this direction is made in section 6 below. Second, the relationship observed between P' and D' may be partly attributable to the effect of the cyclic boundary conditions on correlations between the noise in the two fields. This problem is discussed in section 7.

6) Non-linear coupling

The most obvious flaw in the regression model used in section 5 is the assumption of linear coupling. It is possible that the strength of the coupling between P', T' and D' may depend systematically on the mean state of the atmosphere-ocean system in a particular region.

It is clearly impractical to investigate all possible forms of non-linearity. Only the two types which have already been introduced in the "universal" heating parameterisation $Q'_{(forward\ model)}$ are considered here. If these two forms of non-linearity are allowed, the cost-function to be minimised becomes *(10b)*, and the regression model under investigation becomes *(3b)*, which asserts a relationship between P', $[f_D D]'$ and $[f_T(T - 28°C)]'$. For what functional forms of f_T and f_D does this relationship hold best?

Using the framework already developed, f_T (f_D) are simple step-functions, equal to *1* for total T (D) greater than $28°C$ ($0s^{-1}$), and $f_T = a_T$ ($f_D = a_D$) for T (D) less than $28°C$ ($0s^{-1}$). By adjusting a_T and a_D, giving them the values shown on the horizontal and vertical axes respectively of figure 6, it is possible to scan from fully linear ($a_T = a_D = 1$), through weakly non-linear to strongly non-linear coupling. The linear regression problem (minimising the cost function in *(10b)*) is solved for each (a_T,a_D) pair. Figure 6 shows how the CMC varies with (a_T,a_D). The value of the cost-function varies similarly, but as a statistical measure, this depends on the DOF of the system, which are even less clearly defined in this case than in the problem discussed in section 5.

If non-linear coupling of this form either to SST or to divergence were indicated, then the CMC should peak at some point other than *(1,1)*. It does not appear to do so. Figure 6 therefore fails to provide any positive evidence for either form, although it only provides evidence against strongly non-linear coupling to SST as proposed in, for example, the coupled model of Anderson and McCreary (1985). Adjusting the critical temperature above

and below 28°C makes little difference to this result (provided, of course, it is less than the maximum SSTs observed). Non-linear coupling to divergence, as in the ZC model, cannot be excluded, although there is no indication that it represents a significant improvement on a fully linear scheme. It must, however, be emphasised that these two simple step functions by no means exhaust possible non-linearities.

For all the (a_T,a_D) combinations considered, the "optimum" value of c^2 was found to be negative and significantly different from zero at the 95% level. The implications of this result are discussed in section 8 below. First, however, one further possible reason why the regression model used in section 5 might be misleading must be investigated: dependence of coupling on spatial scale.

7) Sensitivity of results to spatial scale

The coupling between P', D' and T' may not be the same for large-scale anomalies as for small, local anomalies. Moreover, on small spatial scales, correlations between P' and D' may be dominated by coherent relationships between the noise in the two fields, for the following reason. On small scales (high spatial wavenumbers), the term c^2D' in *(3a)* above plays the role of a Laplacian diffusion, as may be seen by eliminating U' and V' from equations *(1)*, *(2)* and *(3a)*, which then reduce to:

$$P' + \frac{c^2}{\alpha^2}\left[- \nabla^2 P' + \frac{\beta(r^2 - \beta^2 y^2)}{r\alpha^2} P'_x + \frac{2\beta^2 y}{\alpha^2} P'_y \right] = - \frac{k_q T'}{r} \qquad (11)$$

where

$$\alpha^2 = r^2 + \beta^2 y^2.$$

For high zonal wavenumbers k, a negative optimum value of c^2, or equivalently a positive correlation between P' and D', should be expected as a consequence of the cyclic zonal boundary conditions imposed. This is because D' is then dominated by $-P'_{xx}$, or in Fourier transform space by $\kappa^2 P'$ (because of the cyclic boundary conditions, only zonally sinusoidal solutions for P' are allowed), where $\kappa = 2\pi k/L$, L being the circumference of the equator. P'_{yy} would also be significant term, but its wavenumber-dependence is less clear. Clearly, P' is positively correlated with $\kappa^2 P'$, and therefore (if only sinusoidal

solutions are allowed) with $-P'_{xx}$. Thus if the regression coefficient between P' and D' were to increase quadratically with zonal wavenumber, this would indicate that the relationship between P' and D' found in section 5 is largely attributable to noise.

To investigate this possibility, the complex discrete Fourier transform of the equatorial monthly mean values of P', D' and T' was obtained, transforming in the zonal direction, again using the SST values in the CAC dataset interpolated over land. Since land comprises less than 20% of the earth's circumference on the equator, this should not unduly affect results relating to low zonal wavenumbers.

This gave, for each zonal wavenumber k, a set of 3 time-series, each containing $2N$ observations, being the real and imaginary Fourier coefficients of P', D' and T' corresponding to that wavenumber for each of the N months. The regression problem discussed in section 5 was then solved for the Fourier coefficients of each zonal wavenumber in turn, minimising C_{3k} in the Fourier transform of *(10c)*, summing over both real and imaginary coefficients.

Problems concerning the true number of DOF of the system do not arise under this procedure. Since only equatorial data are considered, each month's fields are one-dimensional, so the independence of data on different latitudes is not at issue. Each zonal wavenumber has two DOF (amplitude and phase) per month, corresponding to the real and imaginary Fourier coefficients: hence $2N$ DOF per wavenumber.

Figure 7a shows the regression coefficient between P' and T', i.e. the optimum value of $(-k_q/r)$, in the Fourier transform of *(10c)* for the lowest 10 zonal wavenumbers, with error bars showing one standard error on either side of the estimated value. The corresponding regression coefficient which minimises the un-transformed version of *(10c)* using data from all points on the equator (which is equivalent to applying the regression to the Fourier coefficients of all equatorial zonal wave-numbers, weighted by their power spectrum) is also shown, with error bars calculated using the algorithm for DOF described in appendix 2. It is, of course, very similar to the optimum value of $(-k_q/r)$ found in section 5, since the only difference here is a change in the meridional weighting function (only equatorial data are used in figures 7a and 7b). Figure 7b shows the corresponding results for P' and D' $(-c^2/r)$. The 95% confidence limits correspond to approximately 2 standard errors with this sample number.

If *(3a)* represented an adequate regression model for this data, these regression coefficients should not depend systematically on wavenumber. The fact that there clearly is such a dependence provides further evidence that *(3a)* is not an adequate model. More detailed investigation may suggest how the model may be improved. Some qualitative observations are made here.

First, the unexpected positive correlation between P' and D' found in section 5 is not entirely attributable to noise, because the value of the regression coefficient $(-c^2/r)$ is not observed to increase quadratically with wavenumber.

Second, the decrease with wavenumber of the magnitude of the regression coefficient between P' and T' (which is also observed in simple bivariate regression, not shown) indicates that the P' response to SST anomalies is diffusive. This is to be expected, given that the spatial structure of the P' field in figure 2a is smoother than that of the SST field in figure 2b. Some form of diffusion is required in the "thermodynamic" equation linking P' and T' for the relationship between them to be even approximately correct. The term c^2D' in *(3a)* above plays this role, as may be seen from *(11)*. The need for a diffusion term was observed by Lindzen and Nigam (1987), when they found that with c^2 set to zero (zero cumulus uptake time, zero diffusion in *(11)*), the wind response to equatorial SST anomalies was too concentrated on the equator.

Third, however, simple Laplacian-type diffusion as in *(11)* does not seem to be indicated by these observations. If it were, the value of c^2 indicated by the regression coefficients between spectral coefficients of equatorial P' and D' fields (figure 7b) would be positive, at least for those wavenumbers for which the forcing due to SST plays a significant role $(1 \leq k \leq 6)$. As it is, the optimum value of c^2 is found to be either negative, or not significantly different from zero, for all wavenumbers.

8) Implications of $c^2 < 0$

In all of the theoretically-based models considered, P' decreases with D' for a given T'. In the baroclinic-response interpretation, this implies that, for constant forcing due to SST anomalies, an increase in low-level convergence (negative D') induces a positive mid-troposphere geopotential height anomaly which is dispersed by Newtonian cooling. The rate of cooling is held to be proportional to the height anomaly, and thus, in the

equilibrium-response model, to the intensity of convergence: hence, along an isoline of T', $P' = -(c^2/r_t)D' + constant$. The introduction of convergence-forcing feedback may change the magnitude of this coefficient, but it cannot change its sign, or the model becomes unstable, as noted in Zebiak (1986).

In the Lindzen-Nigam interpretation, low-level convergence induces a positive anomaly in the thickness of the boundary layer (and thus the mean boundary-layer pressure) proportional to the characteristic delay in cumulus flux transporting the excess mass convergence upwards out of the boundary layer. Thus in both interpretations, D' is driving P', and some mechanism is invoked whereby the response may be represented by a linear damping on P'.

The results of this analysis suggest a rather different picture. Along an isoline of SST forcing (total and anomalous SST), positive P' anomalies are, more often than not, associated with divergence, suggesting that whatever is controlling the response cannot simply be represented by a linear damping on P'. It is difficult to make sense of this result in terms of a purely sensible-heating-driven model such as that of LN. However, if latent heating effects are considered, the picture becomes clearer. If the contributions of dry static stability and moisture-convergence feedback are separated out, *(3a)* may be rewritten thus:

$$rP' + c_d^2 D' = -k_q T' + \sigma^2 D' \qquad (12)$$

where σ^2 plays the role of Zebiak's convergence-forcing feedback parameter β_z, except that it is independent of D. It has been argued in section 3 that there is no reason in principle why the anomalous latent heating cannot be a linear function of D', and in the absence of any positive evidence for non-linearity (section 6), it seems reasonable to assume that it is.

Without micro-physical observations of processes occurring in the boundary layer, we have no information concerning the individual values of c_d and σ. They are introduced here for heuristic purposes only. However, the above results do suggest information on their sum. From the sign of the regression coefficients between P' and D', it would appear that the optimum "effective value" of c^2 is negative, or equivalently $\sigma^2 > c_d^2$.

Thus the convergence-forcing feedback term in *(12)* appears to be larger than the damping term, making the total response unstable. More precisely, equations *(1)*, *(2)* and *(12)* would have multiple solutions for any given SST field T', and the amplitude of the P'

response to T' would increase quadratically with wavenumber. A simple model relying only on linear damping on P' to control the response would therefore, if the proportionality constant between P' and D' (c^2) was set to the value suggested by the observations, be "unrealisable": its solutions would be multi-valued or unphysical.

9) Some implications for linear models of the tropical atmosphere

This cannot be the whole story, since the real atmosphere is clearly stable on these temporal and spatial scales, and also fairly strongly damped: coupling to SST anomalies tends rapidly towards zero for all zonal wavenumbers greater than 6 (figure 7a). Introducing simple non-linear coupling to T and D does not appear to improve matters, as discussed in section 6, although the correct form of non-linearity may simply not have been identified.

One possibility, not considered here, is that the assumption that Q' is a local function of the SST and convergence is incorrect. For example, the contribution of advective terms to Q' may also be important. In the model of Davey (1985), negative "effective values" of the stability parameter are realisable (corresponding to the case where cooling due to the upward motion of air parcels is less than the rate of latent heat release due to moisture convergence), and the stability of the large-scale response is maintained by the moisture advection term. It is not clear how models involving a significant contribution from non-linear advective terms could be fitted into the overall approach taken here.

A second possibility is that the assumption of uniform coupling (k_q, c^2, f_T and f_D having the same values or functional forms over the whole domain) is incorrect. This is to be pursued in a subsequent study.

A third possibility is that linear, uniform coupling may be assumed, but further terms are required in a model consisting of equations *(1)*, *(2)* and *(12)*. The usual parameterisation of turbulent dissipation has been omitted from *(1)* and *(2)*. Reintroducing it gives:

$$r_m U' - \beta y V' = -P'_x + \nu^2 \nabla^2 U' \qquad (1a)$$

$$r_m V' + \beta y U' = -P'_y + \nu^2 \nabla^2 V' \qquad (2a)$$

Re-analysing the observed winds with these revised momentum equations goes beyond the scope of this study. However, some indication of the effect of turbulent dissipation may be

seen by eliminating U' and V' from equations *(1a)*, *(2a)* and *(12)*. This gives a complicated expression for P' in terms of T' which includes terms proportional to $\nabla^4 P'$. A much simpler alternative parameterisation of turbulent dissipation might therefore be to introduce a biharmonic diffusion term into *(12)* directly, which then becomes:

$$rP' + (c_d^2 - \sigma^2)D' + r\lambda^4 \nabla^4 P' = -k_q T' \qquad (13)$$

which has single-valued solutions for (reasonably smooth) T' fields provided that

$$\lambda^2 > \frac{\sigma^2 - c_d^2}{2r^2}$$

thus allowing the "effective value" of c^2 $(c_d^2 - \sigma^2)$ to be negative.

A model consisting of equations *(1)*, *(2)* and *(13)* would have interesting properties from the perspective of coupled ocean-atmosphere modelling. In particular, it would have a preferred spatial scale of response. A model which only incorporates Laplacian diffusion responds most strongly to wavenumber *1* forcing, and the strength of the response follows an approximately inverse-quadratic decay (following k^{-2}) with increasing wavenumber. Ignoring meridional variations, a model incorporating higher-order dispersion, as in *(13)*, would give a maximum response to equatorial forcing with zonal wavenumber

$$\kappa_{max}^2 = \frac{\sigma^2 - c_d^2}{2r^2\lambda^4}.$$

The scope for adjustment of this most-favoured-wavenumber would be an interesting additional degree of freedom which such a model would possess over existing linear models of the tropical atmosphere. This analysis is only intended to indicate that there may be scope for improvement in linear model atmospheres along the lines suggested. Whether the changes proposed would amount to a genuine improvement would depend on the performance of the forward model, both in response to prescribed SSTs and in coupled experiments, which has not yet been investigated.

10) Summary

Observed wind anomalies during the period 1984 to 1990 were found, to a close approximation, to satisfy the linear damped momentum equations *(1)* and *(2)*. "Filtered winds" (solutions to these equations) were obtained by a least-squares-fit to wind observations (minimising the cost function C_1 in *(4)* using Lagrange multipliers). An optimum value for the mechanical damping rate was obtained *($1*10^{-5}s^{-1}$)* and pressure anomaly fields P' were derived from the filtered winds (section 2).

A similar approach, this time involving a least-squares-fit between the filtered winds and the output of a simple "Gill-type" model atmosphere, consisting of equations *(1)*, *(2)* and *(3a)* with input from observed SST anomalies T', gave reasonable values for either the coupling parameter k_q or the stability parameter c^2, provided the value of the other parameter was specified. However, if both k_q and c^2 were allowed to vary, the cost function (C_2 in *(7)*) had no well-defined minimum: a degeneracy problem (section 3).

An alternative approach was to minimise the r.m.s. difference between "heating fields" Q', reconstructed from the data by fitting winds to the linear momentum equations, and the heating fields suggested by two widely-used models of ocean-atmosphere coupling: the boundary-layer model of Lindzen & Nigam (1987) (LN), and the baroclinic-response model of Zebiak (1986) (ZC). Inspecting patterns in these fields was found to be potentially misleading, since their spatial structure is dominated by divergence terms which cancel each other in the cost-function (C_3 in *(10b)*) to be minimised (section 4).

Fitting model heating fields to derived heating fields, as opposed to fitting model winds directly to wind observations, was shown to be equivalent to asserting that the model should reproduce the observed relationship between P', T' and divergence anomalies D' as well as possible. Making this additional demand is necessary to distinguish between the models, because they all seem to do equally well (or badly) in terms of r.m.s. error in reproducing observed winds. Both qualitative and quantitative analysis (minimising C_3 in *(10c)*) of the relationship between the three variables P', T' and D' suggested an optimum value for the stability parameter c^2 which was, unexpectedly, negative (section 5).

Introducing two widely-used forms of non-linear coupling did not seem to alter this result, and no positive evidence was found to suggest that either was an improvement on a fully linear scheme (section 6). Repeating the regression analysis on Fourier coefficients of

individual zonal wavenumbers indicated that this negative value of c^2 could not simply be attributed to correlations between the noise in the fields (section 7).

In physical terms, $c^2 < 0$ suggests that the lower troposphere is sufficiently unstable that, along an isoline of SST forcing, anomalous low pressure is maintained even in the presence of anomalous convergence and *vice versa*. However, if a negative value of c^2 is inserted into the simple linear model without any further change, model solutions become multi-valued and unphysical (section 8). Three possible solutions to this problem were proposed in section 9: non-linear advective terms, neglected by this analysis, may in fact be playing an important role; the assumption of spatially uniform (although possibly non-linear) coupling may be invalid; or finally, if uniform linear coupling is assumed, the effect of turbulent dissipation must be included in the equations (most simply in the form of a biharmonic diffusion on P') for a stable model to reproduce the observed relationship between P', D' and T'.

It must be emphasised that these results are based on data dominated by only a single ENSO event. There is a clear need to extend the analysis over a longer data-set. However, this initial exercise demonstrates that the application of linear inverse methods in this way can yield interesting information on optimum ranges for parameter values.

Acknowledgments

We wish to thank Klaus Arpe, for providing the wind data-set used, and Maria Ortiz, Brian Weare and Andreas Hense, for advice on statistical methods. The "inverse Gill problem" was previously addressed by Garry Budin, providing a starting point for this research. Conversations with Richard Kleeman and Richard Lindzen also provided a valuable stimulus to this work. Myles Allen was supported in the course of this research by a CASE award through the UK Natural Environment Research Council and the UK Meteorological Office.

Appendix 1: Inverting the linear momentum equations

We approach the problem of identifying the wind field *(U,V)* which best fits (in a least-squares sense) an arbitrary observed wind field (U^0,V^0) and satisfies the linear momentum equations *(1)* & *(2)* above using the method of Lagrange multipliers. Being linear, the method applies to both total and anomaly fields. Primes are omitted here for the sake of clarity. We define the Lagrangian as an integral over the full tropical β-plane from 30°N to 30°S:

$$S = \int_0^{360°} dx\{\ \nu B(U,V,P)_{NS} + \int_{y_S}^{y_N} dy[\ \frac{(U-U^0)^2}{\alpha^2} + \frac{(V-V^0)^2}{\alpha^2} + \lambda(\ rU - \beta yV + P_x\ )^{(I)} + \mu(\ rV + \beta yU + P_y\ )^{(II)}\ ]\}\ (A1)$$

where x and y are the zonal and meridional coordinates respectively; λ, μ and ν are Lagrange multipliers; and $B(U,V,P)_{NS}$ is a function of the solution wind field on the northern and southern boundaries which depends on the boundary conditions specified. B is identically zero, but never needs to be explicitly defined. We define

$$\alpha^2 = r_0^2 + \beta^2 y^2$$

setting $r_0 = 10^{-5}$ Note that, with this value of r_0, $\alpha^2 = r_0^2/w(y)$, where $w(y)$ is a meridional weighting function with a half-width at half maximum of $y_o = 5°$.

$$w(y) = \frac{y_o^2}{(y_o^2 + y^2)}$$

Since the solution fields P, U and V satisfy the linear momentum equations, terms *(I)* and *(II)* in *(A1)* are identically zero everywhere. Thus S is equal to the cost function C_1 in *(4)*, divided by a constant factor r_0^2. By adjusting r_0 we can adjust the half-width of the weighting function. In choosing $r_0 = r$ we could claim to be approximately compensating for the rate of increase of geostrophic winds with latitude, but since there is little physical

justification for choosing one half-width over another, it is important that our results are not sensitive to the value chosen. The functional form of α^2 is for algebraic convenience only.

At the cost-function minimum, partial derivatives of S with respect to U, V and P are identically zero everywhere. Thus, for all y (except $y = y_S$ and $y = y_N$ where partial derivatives with respect to B are non-zero), we have:

$$\frac{\partial S}{\partial U} \equiv 0 = \frac{2(U - U^0)^2}{\alpha^2} + r\lambda + \beta y\mu \qquad (A2)$$

$$\frac{\partial S}{\partial V} \equiv 0 = \frac{2(V - V^0)^2}{\alpha^2} - \beta y\lambda + r\mu \qquad (A3)$$

$$\frac{\partial S}{\partial P} \equiv 0 = -\lambda_x - \mu_y \qquad (A4)$$

By *(A4)*, we may define a stream-function

$$\lambda = -\Psi_y$$
$$\mu = \Psi_x$$

giving

$$U = U^0 - \frac{\alpha^2(\beta y \Psi_x - r\Psi_y)}{2} \qquad (A5)$$

$$V = V^0 - \frac{\alpha^2(\beta y \Psi_y + r\Psi_x)}{2} \qquad (A6)$$

Taking the curl of the linear momentum equations we obtain the linear vorticity balance condition:

$$r(V_x - U_y) + \beta y(U_x + V_y) + \beta V = 0 \qquad (A7)$$

Substituting *(A5)* and *(A6)* into *(A7)* we obtain

$$\alpha^2(r^2 + \beta^2 y^2)(\Psi_{xx} + \Psi_{yy}) + 2\beta^2 y(r^2 + \beta^2 y^2 + \alpha^2)\Psi_y = G^0 \qquad (A8)$$

where

$$G^0 = r(V^0{}_x - U^0{}_y) + \beta y(U^0{}_x + V^0{}_y) + \beta V^0$$

having used the fact that, by our weighting function definition, $(\alpha^2)_y = 2\beta^2 y$.

Northern and southern boundary conditions on Ψ must be specified. If there are no constraints on the solution wind field on the boundaries, then the minimum residual solution is found with the boundary conditions

$$\Psi_{NS} \equiv 0$$

as may be verified by integrating *(A1)* by parts. However, in the "forward model" calculation, where the winds are calculated from a scalar forcing field Q', the usual approach is to specify $V_{NS} \equiv 0$. This yields the meridional boundary conditions

$$\frac{\alpha^2(\beta y \Psi_y + r\Psi_x)_{NS}}{2} \equiv 0$$

Given cyclic zonal boundary conditions, *(A8)* may then be solved directly for Ψ by zonal spectral decomposition, giving a tri-diagonal matrix equation for each spectral coefficient, which may be inverted using Gaussian elimination. U and V are then calculated from Ψ using equations *(A5)* and *(A6)*.

Zonal wavenumber zero (zonal mean quantities) must be treated slightly differently. Since all x derivatives of zonal means are zero, we may eliminate Ψ_y directly from equations *(A5)* and *(A6)* to give, for all y except y_S and y_N:

$$\overline{U} = \overline{U^0} + \overline{\frac{r(-rU^0 + \beta y V^0)}{(r^2 + \beta^2 y^2)}}$$

and

$$\overline{V} = \overline{V^0} - \overline{\frac{\beta y(-rU^0 + \beta y V^0)}{(r^2 + \beta^2 y^2)}}$$

where over-bars indicate zonal mean quantities.

Appendix 2: Estimating degrees of freedom of continuous fields

Significance tests on the results of regression analysis depend on the number of independent observations used in the regression: the number of degrees of freedom (DOF) of the system. When applied to data interpolated onto a grid, this number may be considerably less than the number of data-points, since adjacent data-points do not, in general, constitute independent time-series.

One approach to resolving this problem is to project the data onto the sub-space spanned by a relatively small number of its empirical orthogonal funtions (EOFs), truncating the EOF series using a criterion such as that described in Barnett & Hasselmann (1979), and carrying out the regression analysis on the EOF coefficients. This approach was felt to be inappropriate here, because our overall objective was to investigate regression models, such as *(3a)*, which assert local linear relationships between quantities. If data is projected onto EOFs prior to analysis, then we are no longer testing this locality assumption.

Instead, we assume that some indication of the true number of DOF of the system could be inferred from the spatial structure of the residual fields. If we are testing a local regression model, this amounts to assuming that a given correlation between two fields with very rough structures would provide more evidence in favour of a local regression model than the same correlation observed between two smooth fields.

We also assume that the characteristic spatial scale of the structure of the residual field is a reasonable measure of the "roughness" of the input fields. This spatial scale is estimated by calculating the mean simultaneous correlations between time-series at gridpoints in the residual fields, lagged in space by a specified distance. This space-lag distance is increased, in the zonal and meridional directions in turn, until the correlation drops below *0.1*. The distances at which this occurs are taken to be the characteristic scales of the residual fields in the zonal and meridional directions respectively.

The true number of DOF of the system is then taken to be the E-W width of the fields divided by the zonal scale-length, multipied by the N-S width divided by the meridional scale-length, all multiplied by the number of months in the series (successive months are assumed to constitute independent observation-vectors). Thus if all the grid-points are significantly correlated over all zonal and meridional scales, we have no way of telling if more than one independent observation has contributed to each monthly field: this

algorithm would in that case give a DOF per month of 1. If, at the other extreme, we found adjacent grid-points in the error fields to be uncorrelated, it is reasonable to assume that they constitute independent time-series. In that case the number of DOF per month is assumed to be the same as the number of grid-points.

The algorithm is clearly conservative (i.e. it gives a low estimate of the DOF of the system), since while it is reasonable to suppose that uncorrelated time-series constitute independent sets of observations, the converse is not necessarily true: time-series may be correlated due to the physical properties of the system being analysed, even if independent measurements have been made at each point.

References:

Anderson, D. and McCreary, J., 1985: "Slowly Propagating Disturbances in a Coupled Ocean-Atmosphere Model", *J. Atmos. Sci.*, Vol. 42, No. 6, pp. 615-629

Barnett, T. & Hasselmann, K., 1979: "Techniques of linear prediction with application to oceanic and atmospheric fields in the Tropical Pacific", *Rev. Geophys. Space. Phys.*, Vol. 17, 949-968

Davey, M. & Gill, A., 1987: "Experiments on tropical circulation with a simple moist model", *Quart. J. Roy. Meteor. Soc.*, Vol. 113, pp. 1237-1269

Davey, M., 1985: "Results from a moist equatorial atmosphere model", in Nihoul, J. (ed.), *Coupled Ocean-Atmosphere models*, Elsevier, 1985

Gill, A., 1980: "Some simple solutions for heat-induced tropical circulation", *Quart. J. Roy. Meteor. Soc.*, Vol. 106, pp. 447-462

Goldenberg, S. & O'Brien, J., 1981: "Time and space variability of tropical Pacific wind stress", *Mon. Wea. Rev.*, Vol. 109, 1190-1207

Hirst, A., 1986: "Unstable and Damped Equatorial Modes in Simple Coupled Ocean-Atmosphere Models", *J. Atmos. Sci.*, Vol. 43, No. 6, pp 606-629

Kleeman, R., 1991: "A Simple Model of the Atmospheric Response to ENSO Sea Surface Temperature Anomalies", *J. Atmos. Sci.*, Vol. 48, No. 1, pp 3-18

Lindzen, R., & Nigam, S., 1987: "On the role of sea surface temperature gradients in forcing low level winds and convergence in the tropics", *J. Atmos. Sci.*, Vol. 45, pp. 2440-2458

Matsuno, T., 1966: "Quasi-geostrophic motions in the equatorial area", *J. Met. Soc. of Japan*, Vol. 44, pp. 25-43

Neelin, J., 1988: "A simple model for surface stress and low level flow in the tropical atmosphere driven by prescribed heating", *Quart. J. Roy. Meteor. Soc.*, Vol. 114, pp. 747-770

Neelin, J., 1989: "On the interpretation of the Gill model", *J. Atmos. Sci.*, Vol. 46, pp 2466-2468

Reynolds, R., 1988: "A real-time global sea surface temperature analysis", *J. Climate*, Vol. 1, pp 75-86

Xu, J. & v. Storch, H., 1990: "Predicting the state of the southern oscillation using Principle Oscillation Pattern Analysis", *J. Climate*, Vol. 3, pp 1316-1329

Zebiak, S., 1986: "Atmospheric Convergence Feedback in a Simple Model for El Niño", *Mon. Wea. Rev.*, Vol. 114, pp 1263-1271

Zebiak, S. & Cane, M., 1987: "A Model of El Niño-Southern Oscillation", *Mon. Wea. Rev.*, Vol 115, pp 2262-2278

Zebiak, S., 1990: "Diagnostic Studies of Pacific Surface Winds", *J. Climate*, Vol. 3, pp 1016-1031

Figure 1: Equatorial zonal wind anomalies about the mean annual cycle

Results of linear inverse model: the "filtered" wind data are constrained to conform to the linear damped momentum equations *(1)* and *(2)* (see text), with the mechanical damping rate r optimised at $1*10^{-5}s^{-1}$, boundary conditions $V = 0$ applied on the northern and southern boundaries (30N and 30S), and applying the meridional weighting function w to the cost function to be minimised.

1a) ECMWF analysis: monthly mean winds 1984 to 1990
$U^{0\prime}(y=0)$

1b) Winds filtered to fit linear momentum eqns.
$U'(y=0)$

1c) Error (filtered - analysis)
$U' - U^{0\prime}$

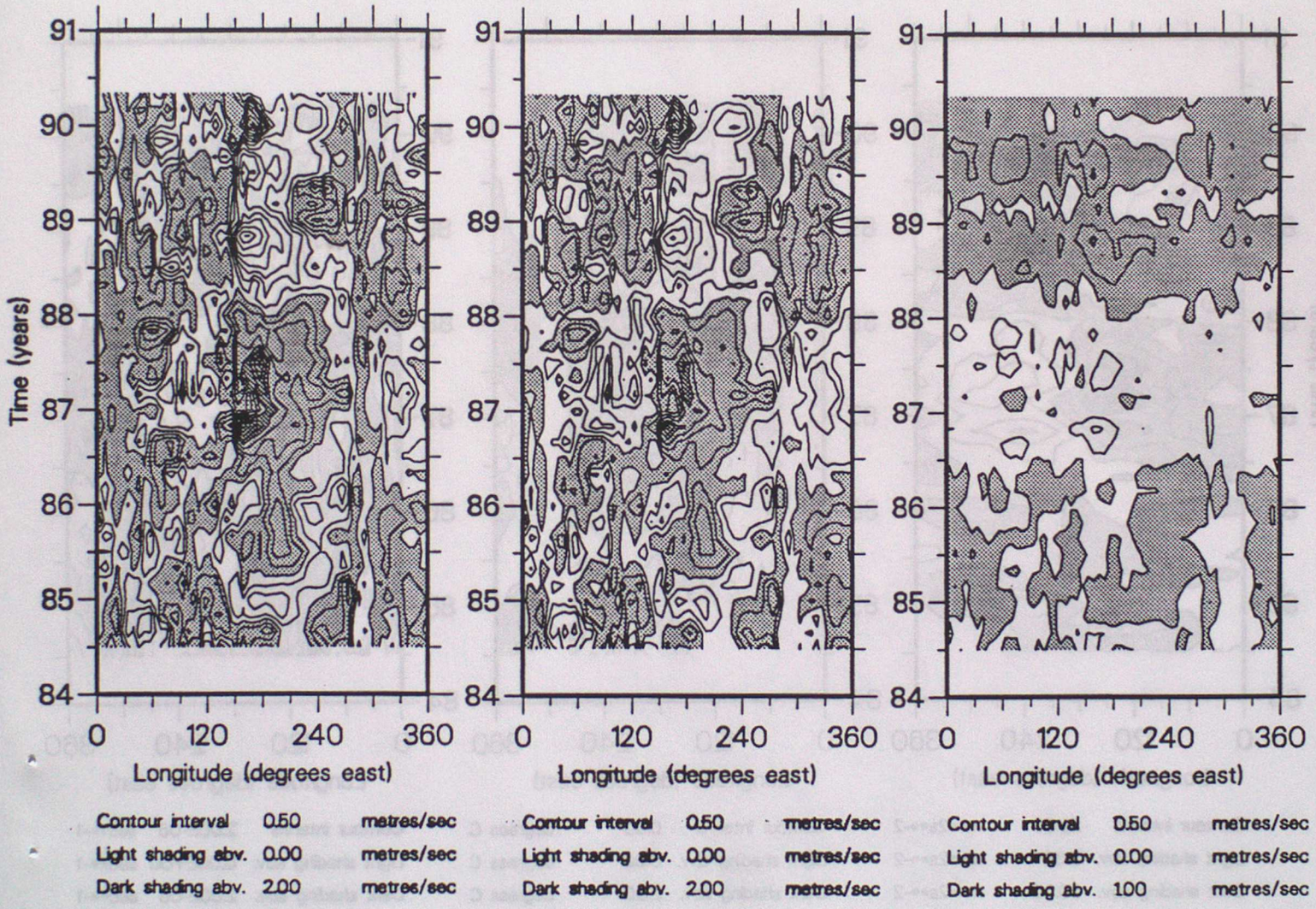

Figure 2: Comparison of equatorial P' field with SST and divergence anomalies

P' derived from the filtered winds (figure 1b) by integrating either *(1)* or *(2)*, compared with SST anomalies from the Climate Analysis Centre dataset, and divergence anomalies calculated from the filtered winds. Note that SST and divergence anomalies are anti-correlated.

2a) Integrated boundary-layer pressure anomalies, P'

2b) Sea-surface temperature anomalies, T'

2c) Divergence anomalies, $D' = U'_x + V'_y$

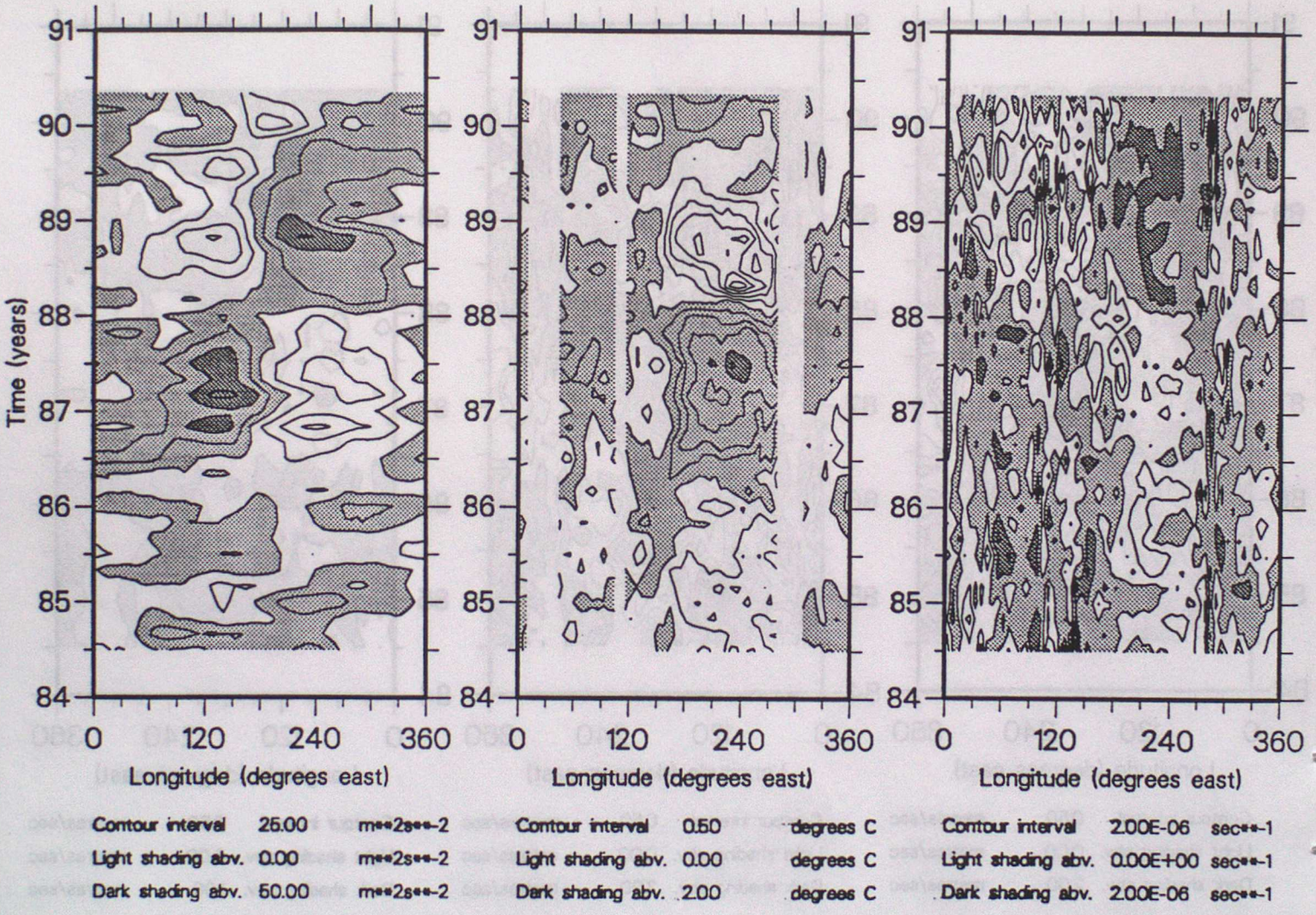

Figure 3: Results of direct "forward model" optimisation

3a) Optimum regression coefficient k_q found to minimise the r.m.s. error in the wind field generated by a linear model atmosphere consisting of equations *(1)*, *(2)*, and *(3a)* with observed SSTs (i.e. minimise C_2 in *(7)*) for a range of values of c^2.

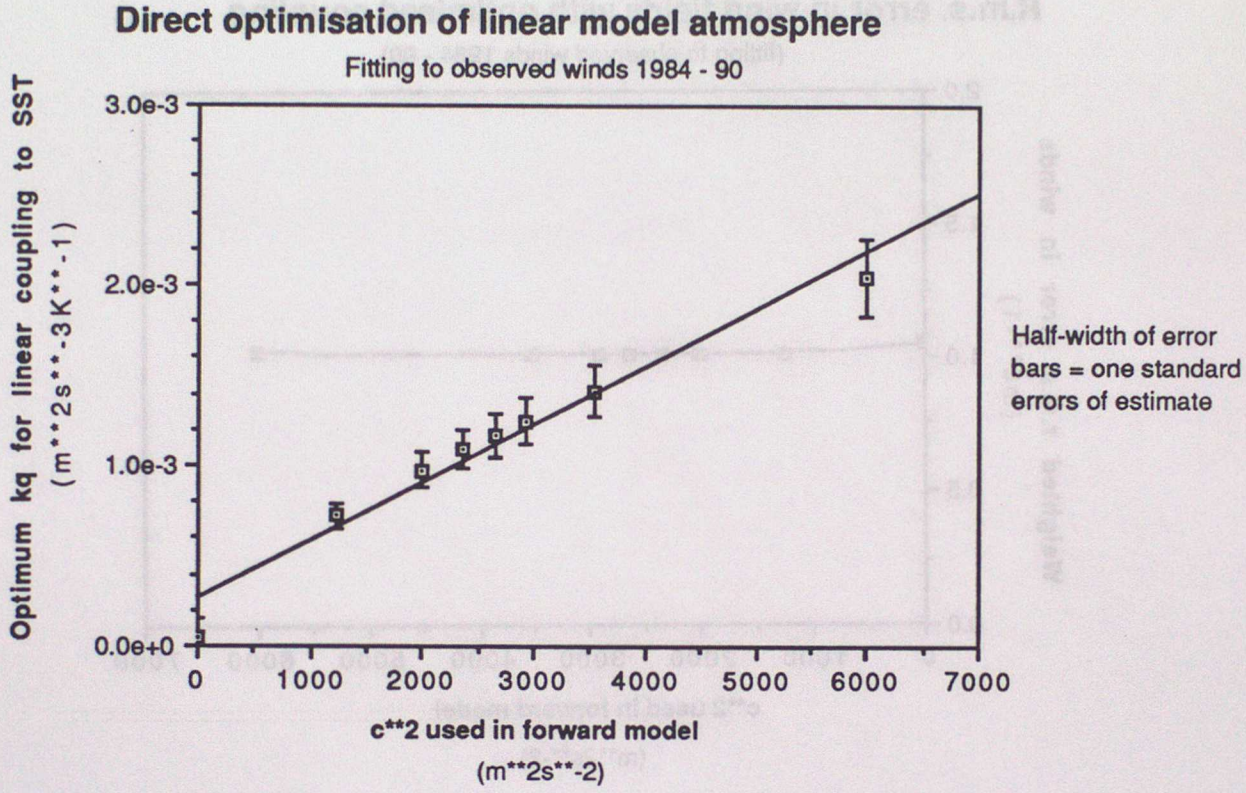

Figure 3: Results of direct "forward model" optimisation, cont.

3b) Variation against c^2 of the r.m.s. error in the wind field generated by a linear model atmosphere with k_q optimised for each value of c^2 (i.e. k_q taking the values shown in figure 3a). Note that C_2 has no well-defined minimum.

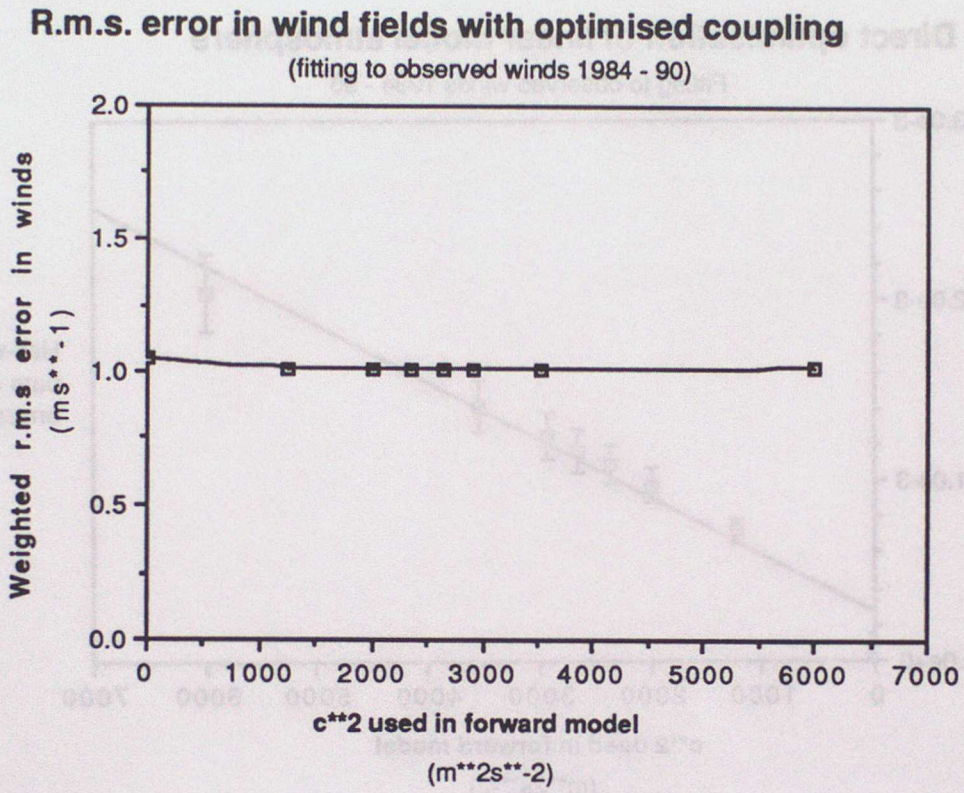

Figure 4: Anomaly fields for January 1987

4a) $Q'_{(inverse\ model)} = -rP' - c_d^2 D'$; with $c_d^2 = 3{,}600 m^2 s^{-2}$ as in the ZC model. Spatial structure is dominated by D'.

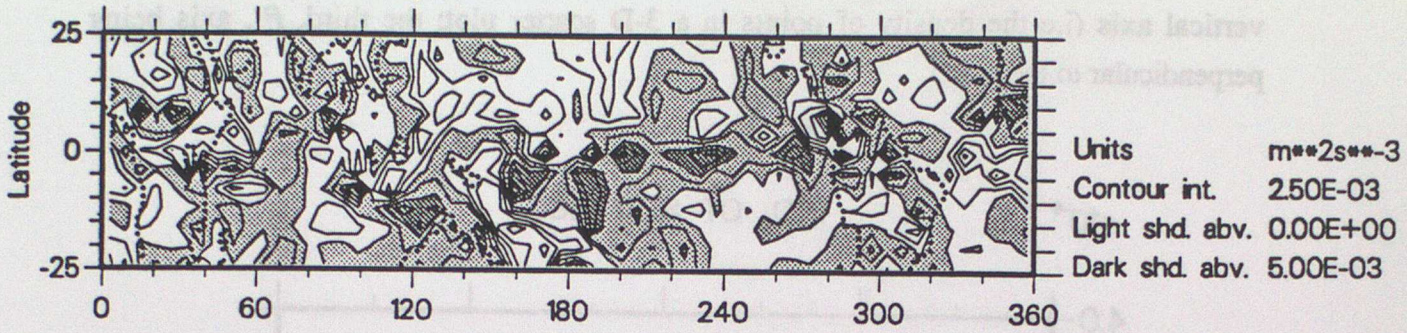

4b) $Q'_{(ZC\ model)} = k_q[f_T(T - T_{cr})]' - c_d^2[\beta_z D]'$; with k_q optimised by linear regression. Spatial structure also dominated by D' in West and Central Pacific.

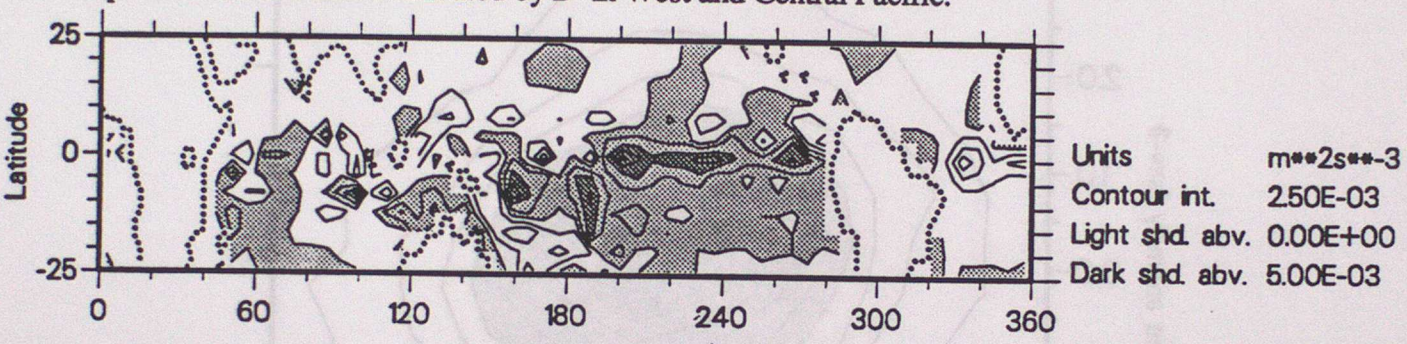

4c) P' generated by the inverse model: no obvious relationship to D', zonal variation along the equator appears more similar to SST anomaly.

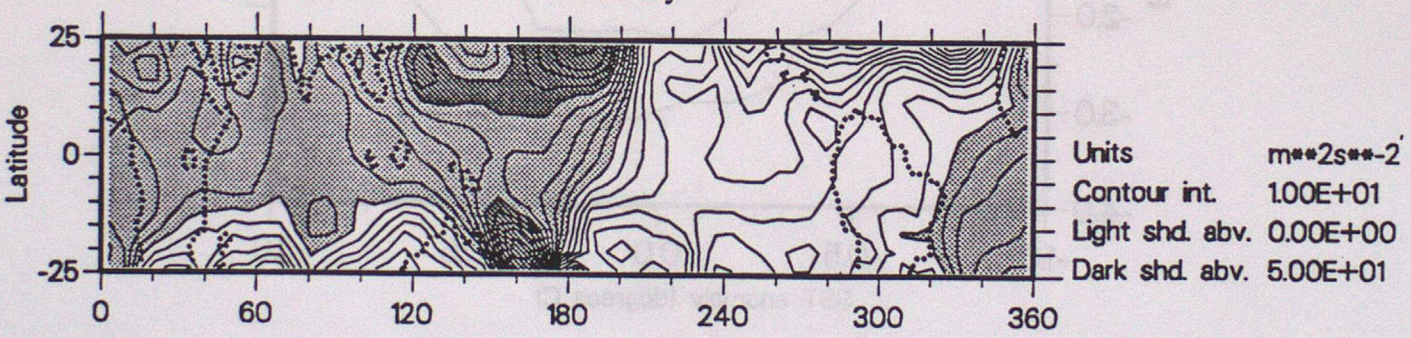

4d) SST anomaly, T'.

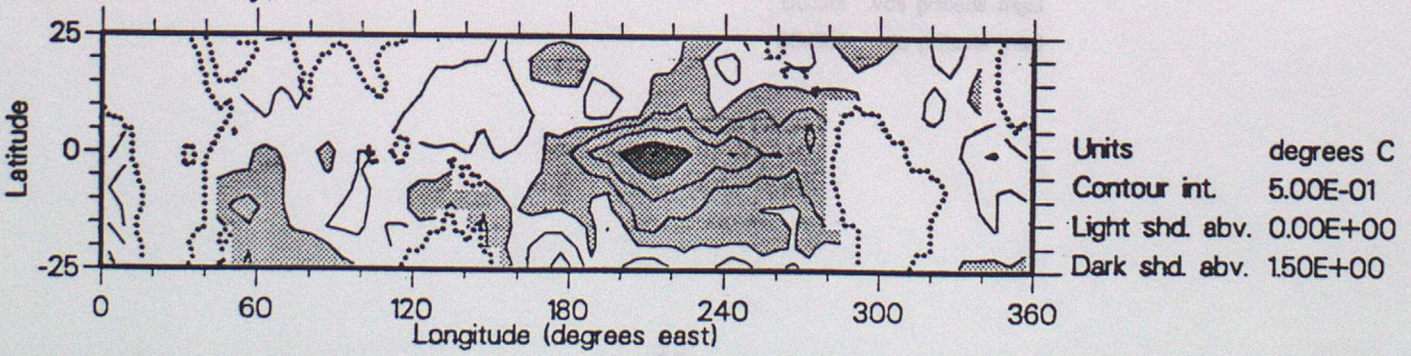

Figure 5: Variation of P' with SST anomalies T' and divergence anomalies D'

5a) The number of samples in which the value of T' was within $+/-0.05°C$ of the value shown on the horizontal axis, and the value of D' was within $+/-2*10^{-7}s^{-1}$ of the value on the vertical axis (i.e the density of points in a 3-D scatter plot: the third, P', axis being perpendicular to the page).

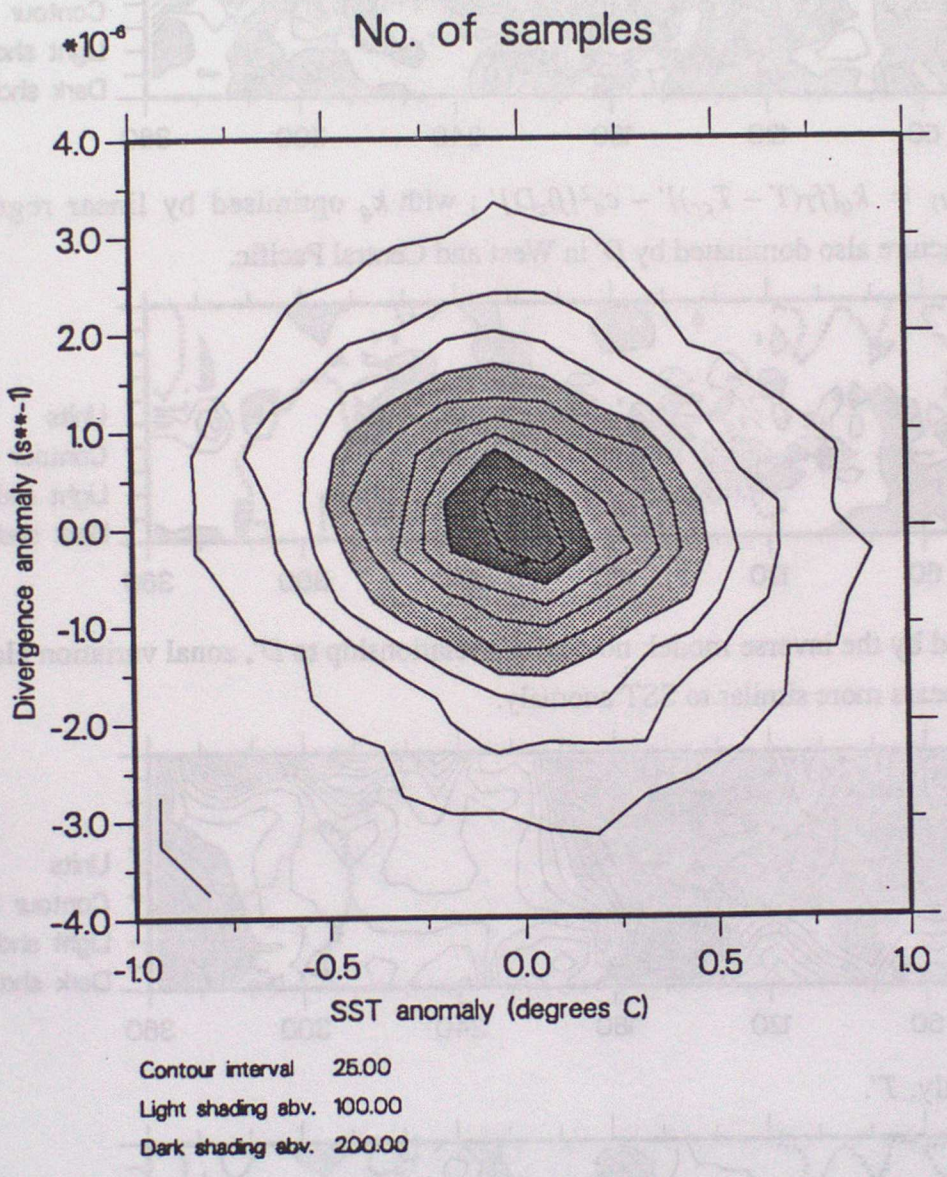

Figure 5: Variation of P' with SST anomalies T' and divergence anomalies D, cont.'

5b) The mean of P' among the samples at the corresponding point in fig. 5a (i.e. a surface passing through the mean, calculated perpendicular to the page, of the points in the 3-D scatter plot). $\partial P'/\partial T' = -k_q/r$ and $\partial P'/\partial D' = -c^2/r$ in the regression model *(3a)*. Note that the surface slopes up from lower right to upper left, indicating $k_q > 0$ and $c^2 < 0$.

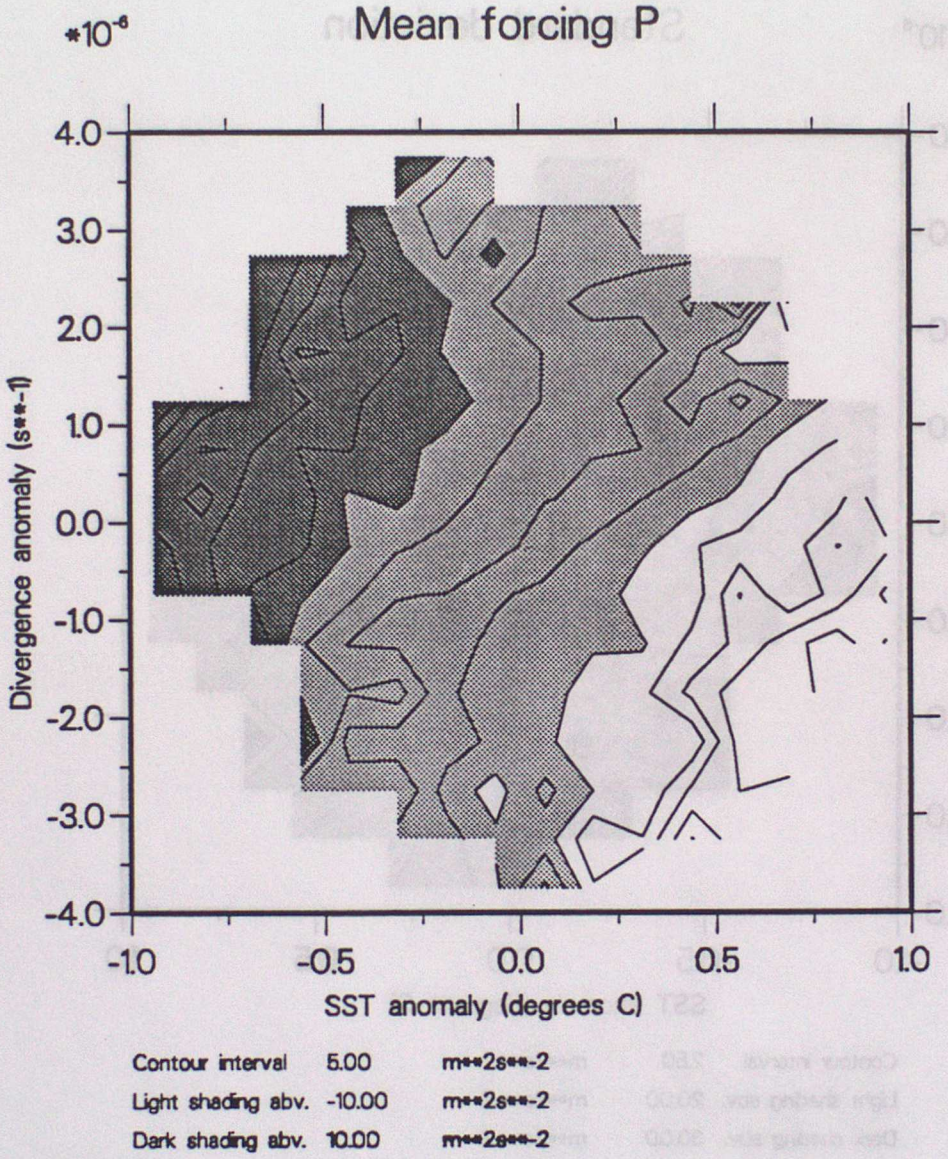

Figure 5: Variation of P' with SST anomalies T' and divergence anomalies D, cont.'

5c) Standard deviation of P' among the samples at the corresponding point in fig. 5a (i.e. the spread, perpendicular to the page, of the points in the 3-D scatter plot). Note that the spread is equal to about 5 contour intervals in fig. 5a.

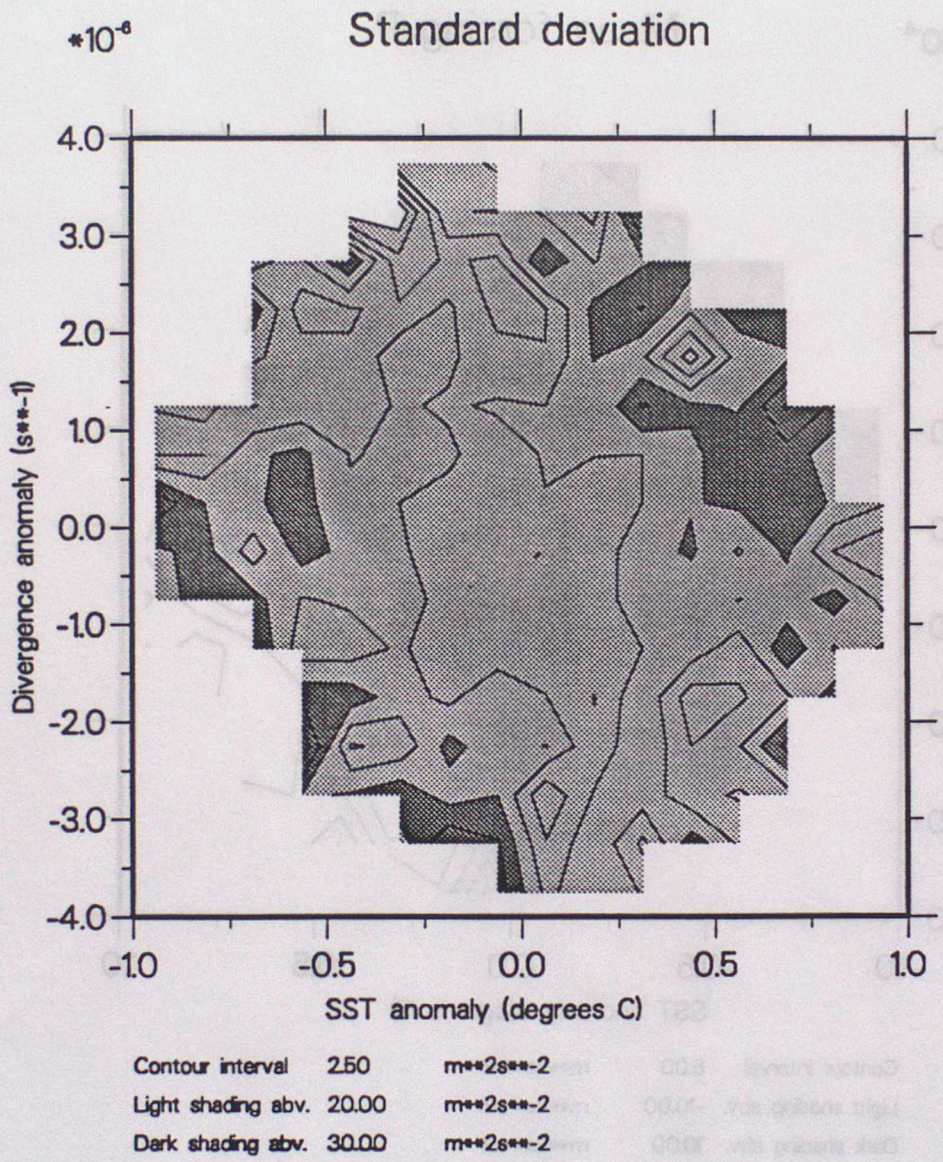

Figure 6: Variation of Coefficient of Multiple Correlation with simple non-linearity functions

Variation of Coefficient of Multiple Correlation between the variables P', $[f_T(T-28°C)]'$, and $[f_D D]'$ against a_T and a_D, being the values of the non-linearity functions f_T and f_D for $T < 28°C$ and $D < 0s^{-1}$ respectively. Higher values of CMC indicate "better" correlation. Note that the correlation obtained by assuming purely linear coupling $(a_T = a_D = 1)$ is as good as any.

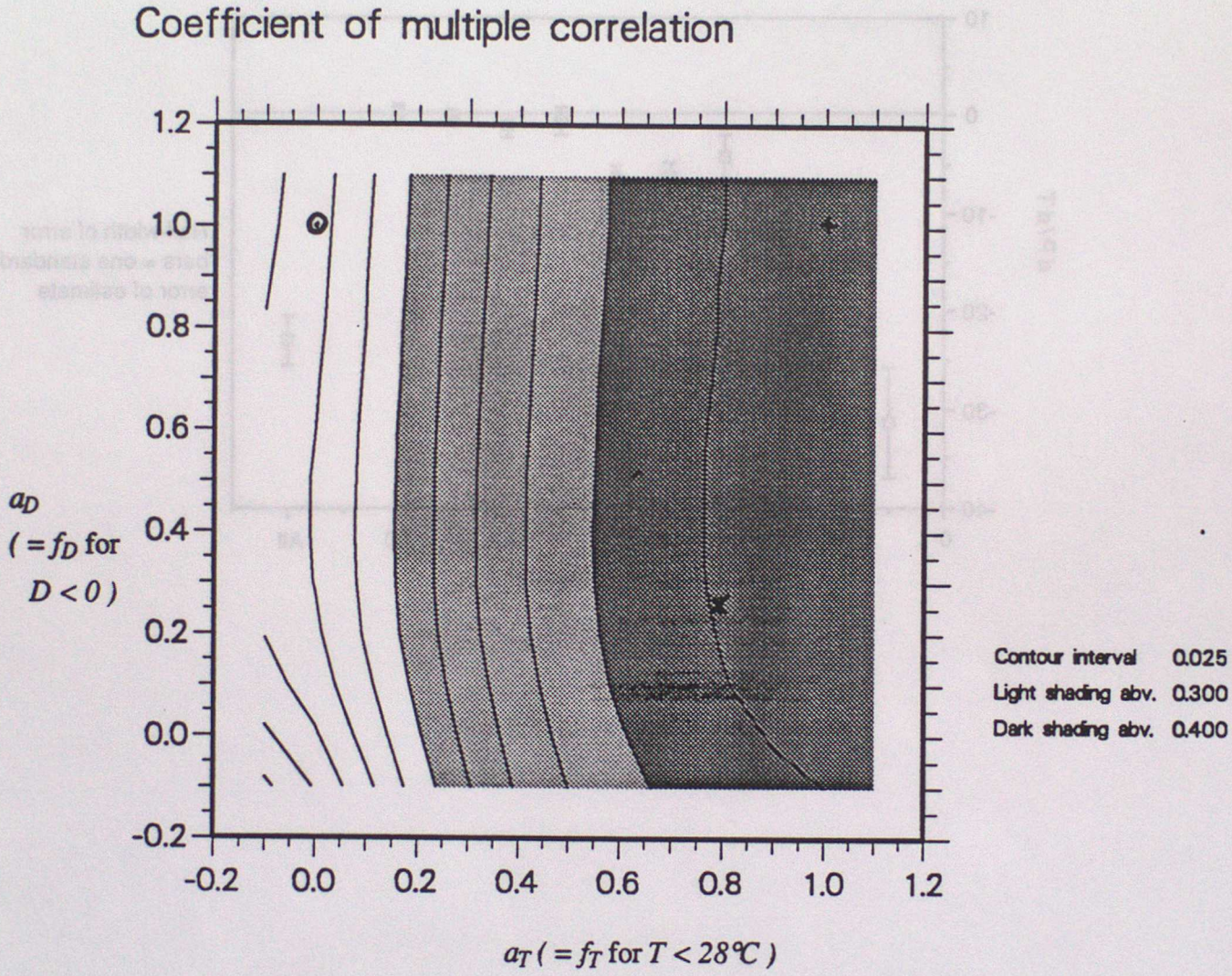

\+ (a_T, a_D) as in Lindzen-Nigam (1987) *(CMC = 0.44)*

× (a_T, a_D) as in Zebiak (1986) *(CMC = 0.43)*

⊙ (a_T, a_D) as in "Dry" Matsuno-Gill model after Anderson & McCreary (1985) *(CMC = 0.24)*

Figure 7: Variation of optimum coupling coefficients with zonal wavenumber

7a) Optimum regression coefficient $\partial P'/\partial T'$ for constant D' ($= -k_q/r$) obtained by trivariate linear regression on real and imaginary Fourier coefficients of individual wavenumbers in the discrete zonal Fourier transform of the equatorial fields P', D' and T'.

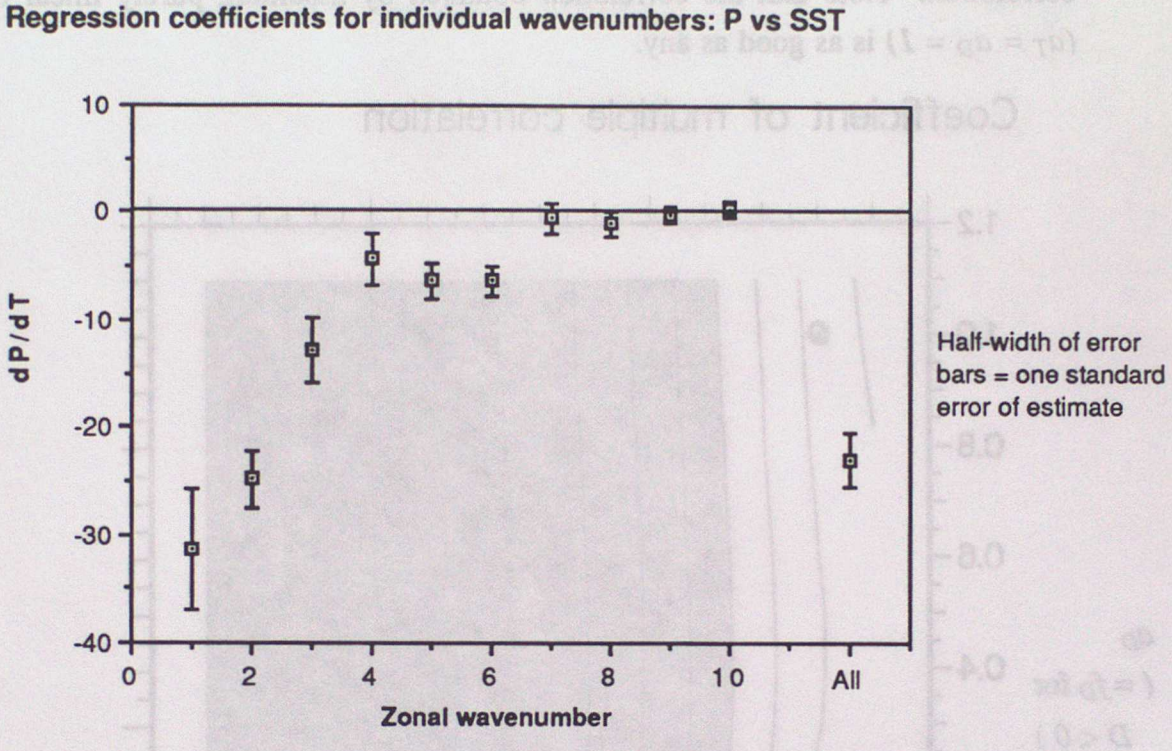

Figure 7: Variation of optimum coupling coefficients with zonal wavenumber – cont.

7b) Optimum regression coefficient $\partial P'/\partial D'$ for constant T' ($= -c^2/r$)

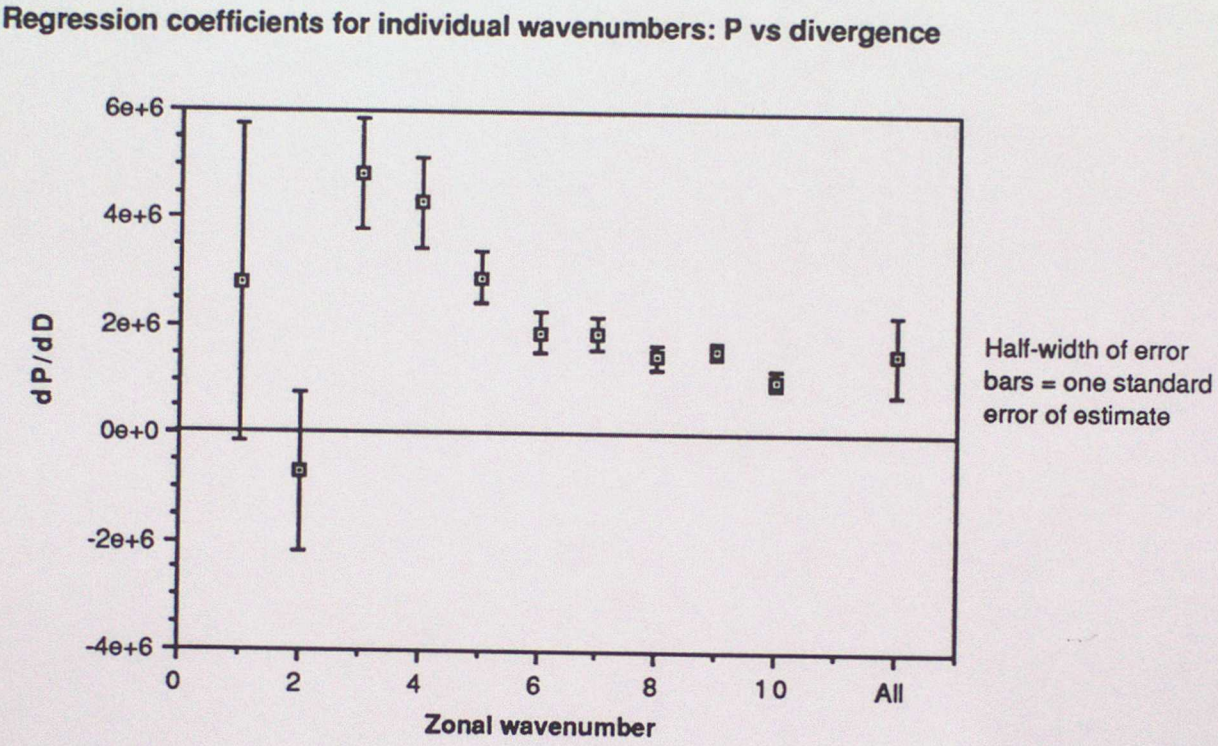

CLIMATE RESEARCH TECHNICAL NOTES

CRTN 1	Oct 1990	Estimates of the sensitivity of climate to vegetation changes using the Penman-Monteith equation. P R Rowntree
CRTN 2	Oct 1990	An ocean general circulation model of the Indian Ocean for hindcasting studies. D J Carrington
CRTN 3	Oct 1990	Simulation of the tropical diurnal cycle in a climate model. D P Rowell
CRTN 4	Oct 1990	Low frequency variability of the oceans. C K Folland, A Colman, D E Parker and A Bevan
CRTN 5	Dec 1990	A comparison of 11-level General Circulation Model Simulations with observations in the East Sahel. K Maskell
CRTN 6	Dec 1990	Climate Change Prediction. J F B Mitchell and Qing-cun Zeng
CRTN 7	Jan 1991	Deforestation of Amazonia - modelling the effects of albedo change. M F Mylne and P R Rowntree
CRTN 8	Jan 1991	The role of observations in climate prediction and research. D J Carson
CRTN 9	Mar 1991	The greenhouse effect and its likely consequences for climate change. D J Carson
CRTN 10	Apr 1991	Use of wind stresses from operational N.W.P. models to force an O.G.C.M. of the Indian Ocean. D J Carrington
CRTN 11	Jun 1991	A new daily Central England Temperature series, 1772-1991. D E Parker, T P Legg and C K Folland
CRTN 12	Jul 1991	Causes and predictability of Sahel rainfall variability. D P Rowell, C K Folland, K Maskell, J A Owen, M N Ward
CRTN 13	Jul 1991	Modelling changes in climate due to enhanced CO_2, the role of atmospheric dynamics, cloud and moisture. C A Senior, J F B Mitchell, H Le Treut and Z-X Li

CLIMATE RESEARCH TECHNICAL NOTES

CRTN 14	Sep 1991	Sea temperature bucket models used to correct historical SST data in the Meteorological Office. C K Folland
CRTN 15	Aug 1991	Modelling climate change, and some potential effects on agriculture in the U.K. P R Rowntree, B A Callander and J Cochrane
CRTN 16	Aug 1991	The Boreal Forests and Climate G Thomas and P R Rowntree
CRTN 17	Aug 1991	Development of a Stratosphere-Troposphere Data Assimilation System. R Swinbank.
CRTN 18	Sep 1991	A study of asynchronous coupling using a simple climate model. M K Davey.
CRTN 19	Sep 1991	The Oceanic Carbon Cycle. N K Taylor
CRTN 20	Nov 1991	Worldwide ocean-atmosphere surface fields in Sahel wet and dry years using provisionally corrected surface wind data. M N Ward
CRTN 21	Dec 1991	Coupled tropical ocean global atmosphere models at the UKMO. M K Davey, C Gordon, S Ineson and S Lawrence
CRTN 22	Dec 1991	Empirical parameterisation of tropical ocean-atmosphere coupling. M Allen, M K Davey, D L T Anderson and P D Killworth